PERFORMANCE OF SPACE TIME TRELLIS CODES OVER NAKAGAMI FADING CHANNELS

by

Kiran Joshi

801263014

Wireless Communication

(ECED)

A thesis submitted in partial fulfillment of the

requirements for the degree of

MASTER OF ENGINEERING

IN

WIRELESS COMMUNICATION

Under the supervision of

Dr. Sanjay Sharma

Professor and Head

(ECED)

ELECTRONICS AND COMMUNICATION ENGINEERING DEPARTMENT

THAPAR UNIVERSITY

(Established under the section 3 of UGC Act, 1956)

PATIALA-147004, PUNJAB, INDIA

JULY, 2014

DECLARATION

I hereby declare that thesis report entitled **"SPACE TIME TRELLIS CODES OVER NAKAGAMI FADING CHANNELS"** for the partial fulfillment of the requirements of the award of degree of Master of Engineering in Wireless Communication at Electronics and Communication Engineering Department of Thapar University (Deemed University), Patiala, Punjab, India is an authentic record of my own work during session of 2012-2014 carried out under the supervision of **Dr. Sanjay Sharma** (Professor & Head), Electronics and Communication Engineering Department.

Date: 02-07-2014

Kiran Joshi
Roll 801263014
Wireless Communications (ECED)

This is to certify that the above statement made by the student is correct to the best of my knowledge and belief.

Date: 02-07-2014

Dr. Sanjay Sharma
Professor and Head
Electronics & Communication Engineering Department
Thapar University, Patiala-147004, (Punjab)

Countersigned by:

Dr. S.K. Mahopatra
Dean of Academic Affairs
Thapar University, Patiala-147004, (Punjab)

ACKNOWLEDGEMENT

I would like to express my gratitude to **Dr. Sanjay Sharma**, Associate Professor, Electronics and Communication Engineering Department, Thapar University, Patiala for his patient guidance and support throughout this work. I am truly very fortunate to have the opportunity to work with him. He provided me great ideas and suggestions during this work and I found his guidance to be extremely valuable.

I am indebted towards my lovely parents and all the family members who continuously support my education and make my path easy to reach up to this peak even in my formidable situations.

I am also thankful to entire faculty and staff members of Electronics and Communication Engineering Department for their unyielding encouragement.

Finally, I am greatly beholden to all my friends, who have graciously applied themselves to the task of helping me with ample morale support and valuable suggestions. I am also thankful to the authors whose works were fruitful in this task. I would also like to extend my gratitude to all those persons who directly or indirectly helped me in the process and contributed towards this work.

-Kiran Joshi-

ABSTRACT

In this technological era thirst for capacity in wireless communication systems has been like sky-rocketing in world-wide day by day. This has been driven by increasing data rate requirements of cellular mobile systems, and demand for wireless internet and multimedia services. As the available radio spectrum is limited, higher data rates can only be achieved by designing more efficient signaling techniques. The research in the field of space-time coding (STC) and multiple-input multiple-output (MIMO) systems has acquired an abundant interest in recent years. MIMO systems apply STC such as space-time block codes (STBC) and space-time trellis codes (STTC). STBC only provides diversity gain but not coding gain later to combat with this STTC were introduced which provide both diversity gain and coding gain with high throughput. STTC is performance criterion based codes, with different modulation techniques and using distribution of codes in constellation this code gives better performance without sacrificing bandwidth, power and other quantities for better transmission of data. Its performance is based on construction of codes, number of transmit and receive antenna and varies with fading channel characteristics.

In this thesis the effect of STTC over fading in MIMO systems which employs the necessary mathematical analysis to consider the achieved capacity performance was analyzed. In this context, flat fading across time and frequency is considered, furthermore, the case of spatial selective fading is examined by considering LOS propagation, with the Rician model and combines both Rician and Rayleigh model to form Nakagami model. It is shown that if number of states of trellis is increased there will be corresponding performance increased. It is shown that if m-factor of Nakagami fading increases up to certain level it improves the performance of the system and if m=1 or Rician fading factor K=0 for special case it corresponds to equivalent Rayleigh fading channel's response. Also, it is shown that if number of transmit antenna were increased at base station for fixed receivers then the burden of increasing receiving antenna will be sort out and also increases throughput. Also for fast fading, 4-state QPSK Nakagami fading channel's performance is better than corresponding Rician and Rayleigh fading channel's performance. It is also derived that for slowly fading, 4-state QPSK Nakagami fading channel's performance is worse than corresponding Rayleigh and Rician fading channel's performance.

DEDICATED
TO MY LATE
GRANDFATHER
MADHAV PRASAD JOSHI

TABLE OF CONTENTS

LIST OF TABLES

LIST OF FIGURES

TERMINOLOGY

AWGN	Additive White Gaussian Noise
BPSK	Binary Phase Shift Keying
BER	Bit Error Rate
BS	Base Staion
CSI	Channel State Information
dB	Decibel
EDC	Euclidean Distance Criteria
FER	Frame Error Rate
ISI	Inter-Symbol Interference
LoS	Line of Sight
ML	Maximum Likelihood
MIMO	Multiple Input Multiple Output
MS	Mobile Station
NLoS	Non-Line of Sight
OFDM	Orthogonal Frequency Division Multiplexing
PDF	Probability Density Function
PEP	Pairwise Error Probability
PSK	Phase Shift Keying
QAM	Quadrature Amplitude Modulation
QPSK	Quadrature Phase Shift Keying
RDC	Rank and Determinant Criteria
Rx	Receiver
SER	Symbol Error Rate
SNR	Signal to Noise Ratio
STBC	Space Time Block Codes
STC	Space Time Codes
STTC	Space Time Trellis Codes
Tx	Transmitter

CHAPTER 1

INTRODUCTION

Introduction

"Imagination is more important than knowledge, for knowledge is limited while imagination embraces the entire world"

-Albert Einstein-

From past few decades people wants delved in to the ocean of information technology in search for high-speed transmission of data on a wireless channel for reliable and spectrally efficient transmission scheme. But their thirst isn't complete for hostility about the wireless channel still it is challenging task. Though emerging of new technologies makes wireless communication an exciting and enthusiastic field. The bandwidth or spectrum availability to service provider is limited and allotment of new spectrum by government is often deliberate in coming. Also, the power requirements of the devices should use as little power as possible to conserve battery life and keep the products small. Thus, the designers for wireless systems face a twin challenges, increase data rates and improve performance while incurring little or no increase in bandwidth or power. Wireless channel is by its nature random and unpredictable, and in general channel error rates are poorer over a wireless channel than over a wired channel.

Recent progresses in wireless communication systems [1] have improved the throughput over wireless channels and also the reliability of wireless communication has been increased. The need to accomplish reliable wireless systems with high spectral efficiency, low complexity and good error performance results in continued research in this field [2]. There is a natural affinity towards getting rid of wires communication if possible. While, this freedom is the main driving force for users, the penalty for this is often lower quality, privacy, security, or lower throughput compared to the equivalent wired solution. Among these wireless designers face the difficult task for limited availability of radio frequency spectrum and time varying problems for wireless channel along with better quality of service (QoS).

Wireless communications systems like cellular mobile communications, internet, multimedia services etc require very high capacity to fulfil the demands of high data rates. These systems must achieve the chosen reliability within the limits of power and frequency spectrum availability, also often in severe channel environments. They need to overcome signal scattering and multipath effects, especially in densely populated urban areas which have many signal obstruction objects. For many communication systems, reliable communication is to be achieved with low probability of detection and interception even in unsympathetic jamming environments. The major objective of communication system design is the effective delivery of information from transmitter to receiver with acceptable number of errors dependent on the application.

Wireless communication systems with multiple transmit and multiple receive antennas [3] can provide high capacity at low probability of bit error with severe low power, even in dense scattering and multipath environments. The solution for achieving high capacity with reliability could include time, frequency and space diversity [4]. These multiple-input multiple-output (MIMO) systems with appropriate space-time codes have been an area of recent research as they hold the promise of ever increasing data rates [3]. The capacities of a MIMO system increased linearly by increasing the number of transmit and receive antennas. The applications of MIMO systems in a frequency selective channel require equalization and other techniques to compensate for frequency selectivity of the channel, which adds complication to these systems. In recent years, orthogonal frequency division multiplexing (OFDM) has been widely used in communications systems to combat frequency selective channels with several wireless communication standards. Communication systems with a MIMO-OFDM combination can significantly improve performance by exploiting the robustness of OFDM to fading environment. It can be enhanced by adding more diversity gain via space time codes (STC). Advances in coding, such as turbo [5] and low density parity check codes (LDPC) [6][7] made it feasible to approach the Shannon capacity limit [4] in systems with a single antenna link. Further advancement in spectral efficiency are available through increasing the number of antennas at both the transmitter and the receiver [1][2].

The theoretical work developed by Telatar [2] and Foschini [1] discuss fundamental capacity limits for transmission over MIMO channels. These capacity limits highlight the possible spectral efficiency of MIMO channels, which grows approximately linearly with

the number of antennas. The capacity is expressed by the maximum achievable data rate for an arbitrarily low probability of error, providing that the signal may be encoded by an arbitrarily long space-time code. It has been proved that the Bell Laboratories Layered Space-Time (BLAST) coding technique [3] can attain the spectral efficiencies up to 42 bits/sec/Hz. This represents a remarkable increase compared to currently achievable spectral efficiencies of 2-4 bits/sec/Hz, in cellular mobile and wireless LAN systems. A MIMO channel can be realized with multi-element array antennas. The International Telecommunication Union (ITU) has formulated a recommendation regarding the direction of future technological developments including fourth generation (4G) communication systems [8]. 4G systems supports data rates in the order of 100 Mbps in the outdoor environment and 1 Gbps in the indoor environment [9]. Any proposed method that can meet these requirements with lower bandwidth will be considered. To support the required large throughputs, wireless communication systems must employ signalling formats and receiver algorithms that provide a significant improve in spectrum efficiency and capacity over current systems. In order to exploit diversity at transmit and receive antennas, MIMO architectures are used to provide multiple data transmission paths. The numbers of inputs refer to the number of antennas used at the transmitter and numbers of outputs refer to the number of antennas used at the receiver.

STC exploits the diversity provided by the MIMO channel in both space (antenna) and time domains, thus significantly increasing the system capacity as well as improving the reliability of the wireless link. The STC can achieve transmit diversity and coding gain compared to spatially uncoded systems without sacrificing bandwidth [11]. STBCs (Space Time Block Codes) and STTCs (Space Time Trellis Codes) are the two main classes of space-time codes. In this thesis we work on STTCs [14]. STTC is a class of signalling techniques that combine the design of the channel code with transmit and optionally receive antenna diversity. In addition to the diversity advantage, a certain amount of coding gain can be achieved by a well-designed STTC.

In this research, we limit the analysis to the case of narrowband channels. Performance of STTCs can be analysed in different fading channels such as Rayleigh, Rician and Nakagami channels.

1.1 Wireless Communication

Wireless communication is the transfer of information between two or more points that are not linked by physical wires and any electrical conductor. Wireless operations permit services, such as long-range communications, that are impossible or impractical to implement with the use of wires. Its performance is mainly governed by wireless channel environment. As compared to the typically static and predictable characteristics of a wired channel, the wireless channel is rather dynamic and unpredictable, which makes an exact analysis often difficult. In recent years, optimization of the wireless communication has become critical with the sky-rocketing growth of mobile communication services and emerging broadband mobile Internet access services. This intact challenging wireless channel for the development of high performance and bandwidth-efficient wireless transmission technology.

The most common wireless technologies use radio. Radio propagation refers to the behaviour of radio waves when they are propagated from source to destination. To refer to telecommunications systems (e.g. radio transmitter and receiver, remote controls etc.) which use some form of energy (e.g. radio waves, acoustic energy, etc.) to transfer information without the use of wires. Information is transferred in this manner over both short and long distances. It includes various types of fixed, mobile, and portable applications, comprising two-way radios, digital assistants (PDAs), cellular telephones, and wireless networking. Such as applications of radio *wireless technology* include GPS units, satellite television, broadcast television, wireless computer hardware, cordless telephones, radio receivers.

With regarding to propagation of waves, radio waves are mainly precious by three different modes of physical phenomena: reflection, diffraction, and scattering [12, 13].

Reflection: It occurs when a propagating electromagnetic wave (EMW) impacts upon an object with very large dimensions compared to the wavelength, for example, surface of the earth and building. It forces the transmit signal power to be reflected back to its origin.

Diffraction: It occurs when the radio path between the transmitter and receiver is blocked by a surface with sharp irregularities shapes or small openings. It appears as a

bending of waves around the small obstacles and spreading out of waves past small openings.

Scattering: It is the phenomena that force the radiation of an electromagnetic wave to deviate from a straight path by one or more obstacles, with small dimensions compared to the wavelength. These obstacles that induces scattering, such as lamp posts, foliage, street signs, and are referred to as the scatters. The intensity of radio wave varies with different environments at different instances of time. Other less common methods of achieving wireless communications includes the use of electromagnetic wireless technologies, such as electric fields, light, magnetic, or the use of sound.

1.2 Literature Review

By means of a clockwork keyed transmitter in 1878, David E. Hughes transmitted radio signals over a few hundred yards.

First wireless telephone chat occurred in 1880, when Alexander Graham Bell and Charles Sumner Tainter invented and patented the photophone, a telephone that conducted audio conversations wirelessly over modulated light beams (which are narrow projections of EMW). In that distant era, when utilities did not yet exist to provide electricity and lasers had not even been imagined in science fiction, there were no practical applications for their invention. Similar to free-space optical communication, the photophone also required a clear line of sight (LoS) between its transmitter and its receiver. It would be several decades before the photophone's principles found their first practical applications in military communications and later in fiber optic communications.

Thomas Edison used a vibrator magnet for induction transmission. In 1888, Edison deployed a system of signalling on the Lehigh Valley Railroad. In 1891, Edison obtained the wireless patent for this method using inductance (U.S. Patent 465,971).

In 1888, Heinrich Hertz demonstrated the existence of electromagnetic waves, the underlying basis of most wireless technology. The theory of electromagnetic waves was predicted from the research of James Clerk Maxwell and Michael Faraday. Hertz demonstrated that electromagnetic waves traveled through space in straight lines, could be transmitted, and could be received by an experimental device.

In late 19th century Italian electrical engineer, Guglielmo Marconi [4] for contribution to wireless telegraphy successfully transmitted the first wireless signal over a distance of one and a half miles by using EMW at frequencies near those of radio frequencies to transmit and receive the signals.

In 1904 the invention of the diode by Fleming and the triode by Lee de Forest in 1906 made possible for long-distance (radio) telephony. John Bardeen, William Shockley, and Walter Brattain invented the transistor which later led to the development of the integrated circuits and paved the way for miniaturization of electronic systems.

With the dawn of such technologies the development of wireless phones began in the 1940s in USA. However, it was not until the 1980s and 1990s that cell phones began to expand as a significant strength in the global market. As the number of cell phone users grew from around few thousand in the 1940s to millions by the 1960s, companies began to have more interest in this global market.

With the beginning of computers and digital signal processing in the 1960's and 1970's, studies in information theory proved incredibly successful. Utilizing Marconi's revolutionary discovery and the technological advancements of the past fifty years, cellular telephone networks prospered in the late Twentieth Century.

The gradual evolution of mobile communication systems follows the quest for high data rates, measured in bits/sec (bps) and with a high spectral efficiency, measured in bps/Hz. The first mobile communications systems were analog and are today referred to as systems of the first generation.

In the early of the 1990s, the first digital systems introduced, denoted as *second generation* (2G) systems. In Europe, the most popular 2G system introduced was the *global system for mobile communications* (GSM), which operated in the 900 MHz or the 1,800-MHz band and supported data rates up to 22.8 kbit/s. Basically GSM is a cellular system [i.e., it typically uses a single *base transceiver station* (BTS), which marks the center of a cell and which serves several *mobile stations* (MS), meaning the users]. In the United States, the most popular 2G system is the *TDMA/136*, which is also a digital cellular system. TDMA stands for time-division multiple access. To accomplish higher data rates, two add-ons were developed for GSM, namely *high-speed circuit switched*

data (HSCSD) and the *general packet radio service* (GPRS), providing data rates up to 38.4 kbit/s and 172.2 kbit/s, respectively.

The demand for yet higher data rates enforced the development of a new generation of wireless systems, the so-called *third generation* (3G). 3G systems are characterized by a maximum data rate of at least 384 kbit/s for mobile and 2 mbit/s for indoors. One of the leading technologies for 3G systems is the now well-known *universal mobile telephone system* (UMTS) [also referred to as *wideband code-division multiplex* (WCDMA) or UTRA FDD/TDD]. UMTS represents an evolution in terms of services and data speeds from today's ''second generation'' mobile networks. As a key member of the global family of 3G mobile technologies identified by the International Telecommunication Union (ITU), UMTS is the natural evolutionary choice for operators of GSM networks, currently representing a customer base of more than 850 million end users in 195 countries and representing over 70% of today's digital wireless market. Japan launched the world's first commercial WCDMA network in 2001, and WCDMA networks are now operating commercially in other countries also.

UMTS is also a cellular system and operates in the 2-GHz band. Compared with the 2G systems, UMTS is based on a novel technology. To yield the 3G data rates, an alternative approach was made with the *enhanced data rates for GSM evolution* (*EDGE*) *concept* which is based on GSM and operates in the same frequency bands. The significantly enhanced data rates are obtained by means of a new modulation scheme, which is more efficient than the GSM modulation scheme. As for GSM, two add-ons were developed for EDGE, namely *enhanced circuit switched data* (ECSD) and the *enhanced general packet radio service* (EGPRS). The maximum data rate of the EDGE system is 473.6 kbit/s, which is accomplished by means of EGPRS. Operators over worldwide are also giving their customers a taste of faster data services with so called 2.5G systems based on GPRS technology, a natural evolutionary steppingstone toward UMTS.

Now, engineers seek to transmit not only voice, but also huge quantities of information over wireless networks. Along with mobile phones the development of wireless internet has also been prominent in the recent decade. For this there is need for coding in wireless system for improving the performance of system. The work done by various researchers in the field of Space Time Codes (STC) applies to offer a substantial coding gain, spectral efficiency, and diversity improvement on fading channels. STC constitutes of Space Time

Block Codes (STBC) and Space Time Trellis Codes (STTC). STTC offer substantial coding and diversity gain both but STBC offer only diversity gain. Driven by the desire to support high data rates for a wide range of bearer services, Tarokh *et al.* proposed STTC codes in 1998 [14]. By jointly designing the FEC, modulation, transmit diversity, and optional receive diversity scheme, they increased the throughput of band-limited wireless channels.

A few months later, Alamouti invented allow-complexity STBC [15], which offers significantly lower complexity at the cost of a slight performance degradation. Alamouti's invention motivated Tarokh *et al.* to generalize Alamouti's scheme to an arbitrary number of transmitter antennas.

Bauch *et al.* Agrawal, Li *et al.* and Naguib *et al.* [16] extended the research of STB and STT codes from considering narrow-band channels to dispersive channels.

In order to enable high data rate transmission over wireless fading channels, recently different transmit diversity techniques have been introduced to benefit from antenna diversity also in the downlink while putting the diversity burden on the base station. In Tarokh *et al.* introduced space–time trellis-coded modulation (STTCM) proposing a joint design of coding, modulation and transmit diversity for flat Rayleigh fading channels. By avoiding destructive superposition after combination of the signals transmitted simultaneously from different antennas STTCM achieves the same, theoretically optimal, diversity advantage as receive diversity.

In 2001 Z. Chen, *Student Member, IEEE,* J. Yuan, *Student Member, IEEE,* and B. Vucetic, *Senior Member, IEEE*, "Improved space-time trellis coded modulation scheme on slow Rayleigh fading channels"[17] Improved codes modified codes proposed by Tarokh *et al.* in to better way for transmitting space time codes, as multilevel codes for improving performance of the system.

In 2001, Gong *et al*. presented the performance of the STTCs over Nakagami fading channels. Nakagami fading channel models are considered more versatile than other channel models.

In July 2007 O. Canpolat, *Student Member, IEEE,* M. Uysal, *Senior Member, IEEE,* and M. M. Fareed, *Life Fellow, IEEE,* Proposed *"*Analysis and Design of Distributed Space-Time Trellis Codes With Amplify-and-Forward Relaying," Distributed codes were designed for relay channels and forward the transmitting signal by superposition of signals, such that strength of signal is enough to fade the effects.

In 2010 Marjan Baghaie A., *Student Member, IEEE,* Philippa A. Martin, *Senior Member, IEEE,* and Desmond P. Taylor, *Life Fellow, IEEE* proposed "Grouped Multilevel Space-Time Trellis Codes" [18] Multilevel coding allows the construction of a high complexity coded signal constellation using simple component codes.

In 2011 Jing Yang, Pingzhi Fan, Trung Q. Duong, and Xianfu Lei, proposed "Exact Performance of Two-Way AF Relaying in Nakagami-m Fading Environment," [21] Since Nakagami fading includes both Rician and Rayleigh fading channel response so performance will be better by considering LoS and NLoS components components of the signal.

In early 2013 Sajjad Beygi, *Student Member, IEEE,* Mohammadmehdi Kafashan, *Student Member, IEEE,* Hamid Reza Bahrami, *Member, IEEE,* Tho Le-Ngoc, *Fellow, IEEE,* and Mehdi Maleki, *Student Member, IEEE* proposed "Space-Time Trellis Codes for Two-Way Relay MIMO Channels With Single-Antenna Relay Nodes," [19] Relay channel allows superposition of transmitted signals from different antenna and amplify and forward signals with multi-antenna source and destination nodes.

In 2013, Ilesanmi B. Oluwafemi and Stanley H. Mneney proposed "Performance of Concatenated Coding Scheme over Nakagami Fading Channels", The concatenation coding scheme with iterative decoding involves convolutional code as the outer code and superorthogonal space-time trellis code (SOSTTC) as the inner code.

1.3 Contribution

We provide some contributions of this thesis which are summarized as follows:-

- We derive explicit, rigorous upper and lower bounds on the performance of STTCs with Pairwise Error Probability (PEP). We use Moment Generating

Function (MGF) to approximate PEP in simpler way. We show how PEP is varying with SNRs, and PEP is increasing with low value of SNR.

- We show that by increasing number of states of trellis code the better will be the performance of the system (i.e. BER Vs SNR). We derive the best modulation technique is using QPSK among all, since it maps constellation points with minimum hamming distance.
- We show that performance of STTC over Rayleigh, Rician and Nakagami fading channels. Among which Nakagami fading resspose is better in fast fading environment and then the both rest of the fading channels response and worse in slow fading environment. We also analyse Nakagami channel response with different values of Nakagami parameter 'm' as we increase value of m from 0.5 to 10 the performance is better and gives high throughput.
- We also establish the relationship among Nakagami parameter 'm' and Rician parameter 'k'. For m=1, in special case Nakagami response tends to Rayleigh response. We derive Nakagami fading response is the combination of Rayleigh and Rician fading response and gives high coding and diversity gain.
- We show the deterioration in the diversity order due to antenna selection is attributed to combined code structure and channel model. We also shows that some coding gain can be achieved by adding more antennas while keeping the number of selected antennas fixed.
- In contrast, when antenna selection is to be considered, one may use STTCs when channel is quasi-static fading. This is due to STBCs does not provide any coding gain although they are very simple to design as compared to STTCs. Also Nakagami fading environment is best suitable for such type of fading.

1.4 Organization

The remaining section of the thesis is outlined as follows:

- In Chapter 2, we review preliminaries and definitions, including wireless channels, MIMO system and its channel capacity.
- In Chapter 3, we introduce a brief introduction to space-time coding. We examine PEP of STCs. We derive upper bounds on the system performance. Several numerical examples and simulation results are also provided which support the mathematical analysis.

- In chapter 4, we derive the STTCs in the different fading channels and compare them. Some numerical examples and simulations were also presented according to mathematical analysis.
- In Chapter 5, we present the response and conclusion of work and suggest some ideas for future work.

CHAPTER 2

BACKGROUND

2.1 Wireless Applications and Challenges

- **Applications**

There are numerous applications of wireless communication is applicable. Radio and television broadcasting is perhaps one of the earliest successful common applications. Satellite communications are other important examples. The success of cellular mobile systems and their appeal to the public resulted in a growing attention to wireless communications in industry and academia. Many researchers concentrated on improving the performance of wireless communication systems and expanding it to other sources of information like images, video, and data. The industry has been keenly involved in establishing new standards. Personal digital cellular (PDC), global system for mobile (GSM) communications, IS-54, IS-95, and IS-136 are some of the early examples of these standards. While they support data services up to 9.6 kbps, they are basically designed for speech. More advanced services for up to 100 kbps data transmission has been evolved from these standards and are called 2.5 generation. Recently, third generation mobile systems are being considered for high bit-rate services. With multimedia transmission in mind, the third generation systems are aiming towards the transmission of 144–384 kbps for fast moving users and up to 2.048 Mbps for slow moving users. It includes the enhanced data for global evolution (EDGE) standard, which is a time division multiple access (TDMA) system and an enhancement of GSM. It also includes two standards based on wideband code division multiple access (CDMA). One is a synchronous system called CDMA2000 and the other one is an asynchronous system named WCDMA. In addition to applications demanding higher bit rates, one can use multiple services in the third-generation standards simultaneously. Nowadays 4G (fourth generation) introduced transmission with 1-100 Mbps which can fulfill demands for huge amount of data transmission.

Another important application that drives the demand for high bit rates and spectral efficiency is wireless local area networks (WLANs). The most successful standard in this area is the IEEE 802.11 class of standards. IEEE 802.11a is based on orthogonal

frequency division multiplexing (OFDM) to transmit up to 54 Mbps of data. Other examples of wireless LAN standards include high performance LAN (HiperLAN) and multimedia mobile access communication (MMAC). Both HiperLAN and MMAC use OFDM. The main purpose of a wireless LAN is to provide high-speed network connections to stationary users in buildings. This is an important application of wireless communications as it provides freedom from being physically connected, portability, and flexibility to network users.

There are many other applications of wireless communications. Cordless telephone systems and wireless local loops are two important examples. Cordless telephone standards include the personal handyphone system (PHS), digital cordless telephone (DECT), and cordless telephone (CT2). Wireless personal area network (PAN) systems are utilized in applications with short distance range. IEEE 802.15 works on developing such standards. Bluetooth is a good example of how to build an ad hoc wireless network among devices that are in the vicinity of each other. The Bluetooth standard is based on frequency hop CDMA and transmits over the 2.45 GHz unlicensed frequency band. The aim of wireless PANs is to connect different portable and mobile devices such as cell phones, cordless phones, personal computers, personal digital assistants (PDAs), pagers, peripherals, and so on.

- **Challenges**

While various applications have different specifications and use different wireless technologies, most of them face similar challenges. Some of the challenges in wireless communications are:

- a need for high data rates;
- mobility;
- quality of service;
- portability;
- interference from other users;
- connectivity in wireless networks;
- privacy/security.

Many of the demands, for example the need for high data rates and the quality of service, are not unique to wireless communications. But, some of the challenges are specific to

wireless communication systems. For example, the portability requirement results in the use of batteries and the limitation in the battery life creates a challenge for finding algorithms with low power consumptions. This requires special attention in the design of transmitters and receivers. Another example of challenges in wireless communications is the connectivity in wireless networks. The power of the received signal depends on the distance between the transmitter and the receiver. Therefore, it is important to make sure that if, because of the mobility of the nodes, their distance increases, the nodes remain connected. Also, due to the rapidly changing nature of the wireless channel, mobility brings many new challenges into the picture. In a wired system, the communication environment is more under control and the interference is less damaging. While the demand for data rates and the performance of the signal processors increase exponentially, the spectrum and bandwidth are limited. The limited bandwidth of the wireless channels adds increases impairment.

Researchers face many challenges to satisfy such high expectations through the narrow pipeline of wireless channels. The first step to solve these problems is to understand the behaviour of the wireless channel. This is the main topic of the next section.

2.2 Wireless Channels

The performance of wireless communication systems is mainly governed by the wireless channel environment. As opposed to the typically static and predictable characteristics of a wired channel, the wireless channel is rather dynamic and unpredictable, which makes an exact analysis of the wireless communication system often difficult. In recent years, optimization of the wireless communication system has become critical with the rapid growth of mobile communication services and emerging broadband mobile Internet access services. In fact, the understanding of wireless channels will lay the foundation for the development of high performance and bandwidth-efficient wireless transmission technology. Figure 2.1 shows the typical Additive white Gaussian noise (AWGN) in which the only impairment to communication is a linear addition of white noise with a constant spectral density (expressed as watts per hertz of bandwidth) and a Gaussian distribution of amplitude.

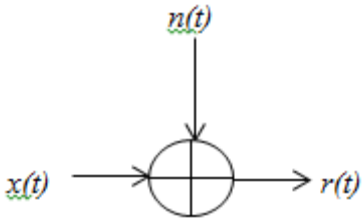

Figure 2.1. AWGN Channel Model.

The model may be described mathematically by considering signal transmission as

$$r(t) = x(t) + n(t) \tag{2.1}$$

where, at time t, $r(t)$ and $x(t)$ are the received and transmitted signals respectively and $n(t)$ is the noise, represented as a sample function from a Gaussian random process with zero mean and variance N_0. The noise $n(t)$ is assumed to be independent of the signal $r(t)$.

2.2.1 Diversity

In the case of severe attenuation of the transmitted signal due to multipath (or fading channels), it becomes impossible for the receiver to determine the transmitted signal unless additional independent replicas of the transmitted signal can be supplied to the receiver. This redundancy is called diversity. This is considered as single most important mechanism for reliable wireless communications. There are several techniques for achieving diversity i.e., frequency diversity, spatial (antenna) diversity and temporal diversity.

Frequency Diversity: Signals transmitted on different frequencies induce different multipath structures. In frequency diversity the information signal is transmitted on more than one carrier frequency. In this way replicas of the transmitted signals are supplied to the receiver in the form of redundancy in the frequency domain.

Temporal Diversity: In temporal (or time) diversity, replicas of the information signal are transmitted in different time slots so that multiple, uncorrelated versions of the signal will be received.

Spatial Diversity (Antenna Diversity): Spatial diversity is one of the most popular forms of diversity used in wireless communication systems. Multiple and spatially

separated antennas are employed to transmit or receive uncorrelated signals. Antenna separation should be at least half of the carrier wavelength to ensure sufficiently uncorrelated signals at the receiver.

2.2.2 Fading

The fading phenomenon in the wireless communication channel was initially modelled for HF (High Frequency, 3-30MHz), UHF (Ultra HF, 300-3000 GHz), and SHF (Super HF, 3-30 GHz) bands in the 1950s and 1960s. Currently, the most popular wireless channel models have been established for 800MHz to 2.5 GHz by extensive channel measurements in the field. These include the ITU-R standard channel models specialized for a single-antenna communication system, typically referred to as a SISO (Single Input Single Output) communication, over some frequency bands. Meanwhile, spatial channel models for a multi-antenna communication system, referred to as the MIMO (Multiple Input Multiple Output) system, have been recently developed by the various research and standardization activities such as IEEE 802, METRA Project, 3GPP/3GPP2, and WINNER Projects, aiming at high-speed wireless transmission and diversity gain. The fading phenomenon can be broadly classified into two different types: large-scale fading and small-scale fading. Large-scale fading or attenuation occurs as the mobile moves through a large distance. It is caused by path loss of signal as a function of distance and shadowing by large objects such as buildings, intervening terrains, and vegetation. Shadowing is a slow fading process characterized by variation of median path loss between the transmitter and receiver in fixed locations. In other words, large-scale fading is characterized by average path loss and shadowing. On the other hand, small-scale fading refers to rapid variation of signal levels due to the constructive and destructive interference of multiple signal paths (multi-paths) when the mobile station moves short distances. Depending on the relative extent of a multipath, frequency selectivity of a channel is characterized (e.g., by frequency-selective or frequency flat) for small-scaling fading. Meanwhile, depending on the time variation in a channel due to mobile speed (characterized by the Doppler spread), short term fading can be classified as either fast fading or slow fading. Figure 2.2 classifies the types of fading channels.

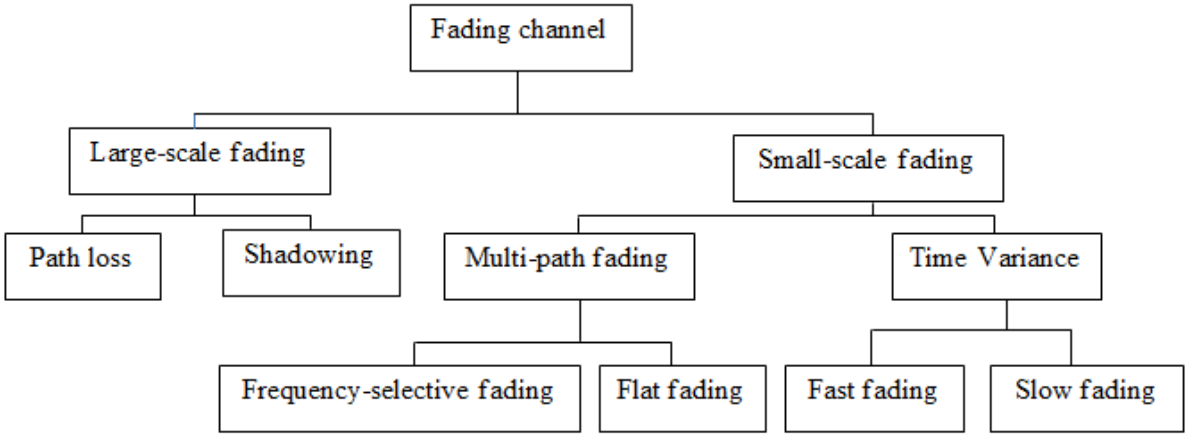

Figure 2.2. Classification of fading channels.

We have classified fading channels based on their multipath time delay into flat and frequency selective and based on Doppler spread into slow and fast. These two phenomena are independent of each other and result in the following four types of fading channels.

- Flat Slow Fading or Frequency Non-Selective Slow Fading: When the bandwidth of the signal is smaller than the coherence bandwidth of the channel and the signal duration is smaller than the coherence time of the channel.
- Flat Fast Fading or Frequency Non-Selective Fast Fading: When the bandwidth of the signal is smaller than the coherence bandwidth of the channel and the signal duration is larger than the coherence time of the channel.
- Frequency Selective Slow Fading: When the bandwidth of the signal is larger than the coherence bandwidth of the channel and the signal duration is smaller than the coherence time of the channel.
- Frequency Selective Fast Fading: When the bandwidth of the signal is larger than the coherence bandwidth of the channel and the signal duration is larger than the coherence time of the channel.

2.3 MIMO System Model

MIMO, uses multiple antennas at both the transmitter and receiver to improve communication performance. MIMO technology has attracted attention in wireless communications, because it offers significant increases in data throughput and link range without additional bandwidth or increased transmit power. It achieves this goal by

spreading the same total transmit power over the antennas to achieve an array gain that improves the spectral efficiency (more bits per second per hertz of bandwidth) or to achieve a diversity gain that improves the link reliability (reduced fading). MIMO schemes that assume the channel knowledge is only available at the receiver have in particular attracted a lot of research attention [6].

MIMO modulation schemes with receive-only channel knowledge are mainly of two types, diversity systems and spatial multiplexing systems. Diversity modulation, or space-time coding [11,12], uses code words designed to maximize the diversity advantage of the transmitted information. Such codes tend to maximize diversity gain at the expense of some loss in available capacity. Spatial multiplexing or Bell Labs Layered Space Time (BLAST) type systems [1], on the other hand, transmit independent data streams from each transmitting antenna, allowing spectral efficiency to be achieved at the expense of a loss in diversity advantage for a fixed number of receive antennas. The original BLAST structure was developed by Foschini [8] which uses a multi-element antenna array at both the transmitter and receiver, where every antenna transmits an independent sub stream of data. Advanced signal processing at the receiver is used to estimate and decode the received signal blocks. A BLAST system requires more receive than transmit antennas and a rich scattering environment, which often occurs indoors. Vertical-BLAST (V-BLAST) and Diagonal-BLAST (D-BLAST) [8] are the two major classes of BLAST transmission formats.

Initially MIMO was proposed for indoor WLANs and fixed wireless access networks. However, it has since found wider applications and some practical MIMO systems have been built and experimentally tested in industry. MIMO is an important part of modern wireless communication standards such as IEEE 802.11n (Wi-Fi), 4G, 3GPPLTE, WiMAX and HSPA+. MIMO technology can be used in non-wireless communications systems. One example is the home networking standard ITU-T G.9963, which defines a power line communications system that uses MIMO techniques to transmit multiple signals over multiple AC wires (phase, neutral and ground). While the correlation-based channel model can be implemented with a spatial correlation matrix for the spatial channel, temporal correlation must also be generated independently by using the specified Doppler spectrum. On the other hand, the ray-based channel model combines the multiple rays distributed in the angular domain for the given Power Azimuth Spectrum (PAS).

This requires neither Doppler spectrum nor spatial correlation matrix, but rather involves a complex computational operation.

2.3.1 Transmission Model for MIMO Channels

We consider a communication system, where *N* signals are transmitted from *N* transmitters simultaneously. For example, in a wireless communication system, at each time slot *t*, signals $\mathbf{C}_{t,n}$, n = 1, 2, …, *N* are transmitted simultaneously from *N* transmit antennas. The signals are the inputs of a MIMO channel with *M* outputs. Each transmitted signal goes through the wireless channel to arrive at each of the *M* receivers. In a wireless communication system with *M* receive antennas; each output of the channel is a linear superposition of the faded versions of the inputs perturbed by noise. Each pair of transmit and receive antennas provides a signal path from the transmitter to the receiver. The coefficient $\alpha_{n,m}$ is the path gain from transmit antenna *n* to receive antenna *m*. Figure 1 depicts a baseband discrete-time model for a flat fading MIMO channel. Based on this model, the signal $r_{t,m}$, which is received at time *t* at antenna *m*, is given by

$$r_{t,m} = \sum_{n=1}^{N} \alpha_{n,m}\, \mathbf{C}_{t,n} + \eta_{t,m} \tag{2.2}$$

where $\eta_{t,m}$ is the noise sample of the receive antenna *m* at time *t*. Based on (2.2), a replica of the transmitted signal from each transmit antenna is added to the signal of each receive antenna. Although the faded versions of different signals are mixed at each receive antenna, the existence of the *M* copies of the transmitted signals at the receiver creates an opportunity to provide diversity gain. If the channel is not flat, the received signal at time *t* depends on the transmitted signals at times before *t* as well. The result is an extension to the case of one transmit and one receive antenna. In this thesis, we only consider the case of narrowband signals for which the channel is a flat fading channel. Another important factor in the behaviour of the channel is the correlation between different path gains at different time slots. There are two general assumptions that correspond to two practical scenarios. First, we assume a quasi-static channel, where the path gains are constant over a frame of length T' and change from frame to frame. In most cases, we assume that the path gains vary independently from one frame to another. Another assumption is to

consider a correlation between the fades in adjacent time samples. One popular example of such a second-order model is the Jakes model [43].

The value of T'dictates the slow or fast nature of the fading. If a block of data is transmitted over a time frame T that is smaller than T', the fading is slow. In this case, the fades do not change during the transmission of one block of data and the values of path gains in (2.1) are constant for every frame. On the other hand, in a fast fading model, the path gains may change during the transmission of one frame of data, $T \gg T'$.

To form a more compact input-output relationship, we collect the signals that are transmitted from N transmit antennas during T time slots in a $T \times N$ matrix, $\mathbf{C}$ as;

$$\mathbf{C} = \begin{pmatrix} C_{1,1} & C_{1,2} & \cdots & C_{1,N} \\ C_{2,1} & C_{2,2} & \cdots & C_{2,N} \\ \vdots & \vdots & \ddots & \vdots \\ C_{T,1} & C_{T,2} & \cdots & C_{T,N} \end{pmatrix} \tag{2.3}$$

Similarly, $T \times M$ received matrix $\mathbf{r}$ that includes all received signals during T time slots.

$$\mathbf{r} = \begin{pmatrix} r_{1,1} & r_{1,2} & \cdots & r_{1,M} \\ r_{2,1} & r_{2,2} & \cdots & r_{2,M} \\ \vdots & \vdots & \ddots & \vdots \\ r_{T,1} & r_{T,2} & \cdots & r_{T,M} \end{pmatrix} \tag{2.4}$$

Then, assuming $T < T'$, gathering the path gains in an $N \times M$ channel matrix $\mathbf{H}$

$$\mathbf{H} = \begin{pmatrix} \alpha_{1,1} & \alpha_{1,2} & \cdots & \alpha_{1,M} \\ \alpha_{2,1} & \alpha_{2,2} & \cdots & \alpha_{2,M} \\ \vdots & \vdots & \ddots & \vdots \\ \alpha_{N,1} & \alpha_{N,2} & \cdots & \alpha_{N,M} \end{pmatrix} \tag{2.5}$$

results in the following matrix form of (2.6):

$$\mathbf{r} = \mathbf{C} \cdot \mathbf{H} + \mathcal{N} \tag{2.6}$$

where $\mathcal{N}$ is the $T \times M$ noise matrix defined by (2.7).

$$\mathcal{N} = \begin{pmatrix} \eta_{1,1} & \eta_{1,2} & \cdots & \eta_{1,M} \\ \eta_{2,1} & \eta_{2,2} & \cdots & \eta_{2,M} \\ \vdots & \vdots & \ddots & \vdots \\ \eta_{T,1} & \eta_{T,2} & \cdots & \eta_{T,M} \end{pmatrix} \tag{2.7}$$

Different path gains may be independent from each other, that is $\alpha_{n,m}$ is independent. We assume a quasi-static slow fading model such that the noise samples $\eta_{t,m}$ are independent samples of a zero-mean circularly symmetric complex Gaussian random variable. This is an additive white Gaussian noise (AWGN) assumption for a complex baseband transmission. The noise samples, channel path gains, and transmitted signals are independent from each other. Also, the bandwidth is narrow enough such that the channel is flat over a band of frequency. Such a channel is called frequency non-selective and the channel matrix is constant over the frequency band of interest. In the sequel, we use the quasi-static, non-frequency selective assumptions unless we mention otherwise.

Let us denote the average power of the transmitted symbols, $C_{T,N}$ by E_s. Also, let us assume that the variance of the zero-mean complex Gaussian noise is $N_0/2$ per dimension. Normalizing E_s and N_0 is to use a constellation with an average power of one for transmission symbols and unit-power noise samples. In this case, a normalization factor is considered in the input-output relationship of the MIMO channel as

$$\mathbf{r} = \sqrt{\frac{\gamma}{N}}\mathbf{C}.\mathbf{H} + \mathcal{N} \tag{2.8}$$

where γ is the received SNR.

2.3.2 MIMO Channel Capacity

We assume that the receiver knows the realization of the channel i.e. it knows both **r** and **H**. For the transmitter, we study two cases.

- The transmitter does not know the realization of the channel; however, it knows the distribution of **H**. This corresponds to an open-loop system as depicted in Figure 2.3(a).
- The transmitter knows the realization of the channel. This corresponds to a closed-loop system as depicted in Figure 2.3(b).

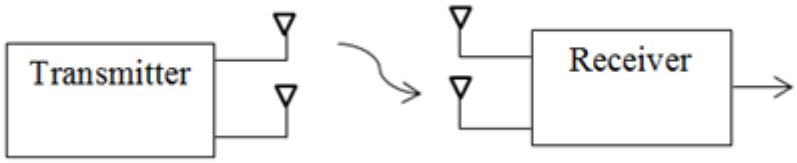

(a)

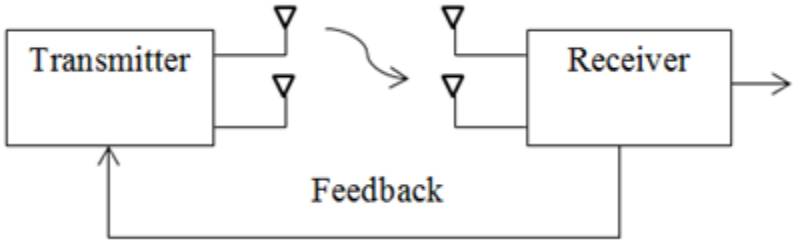

(b)

Figure 2.3. Block diagram of (a) open-loop and (b) closed-loop multiple-input multiple-output systems.

We use a quasi-static block fading model. Under such a model, the channel path gains are fixed during a large enough block such that information theoretical results are valid. The values of path gains change from block to block based on a statistical model, for example a Rayleigh fading channel model. The resulting capacity of the channel is a random variable because the capacity is a function of the channel matrix **H**. The distribution of the capacity is determined by the distribution of the channel matrix **H**. The total transmitted power is kept the same for different numbers of transmit antennas to make a fair comparison. Figure 2.4 shows the MIMO channel capacity(bits/sHz) vs SNR (dB) with 2-tx and 2-rx antenna. The distribution of capacity in Rayleigh fading channel model describes approximately linear with SNR which is shown in figure 2.4.

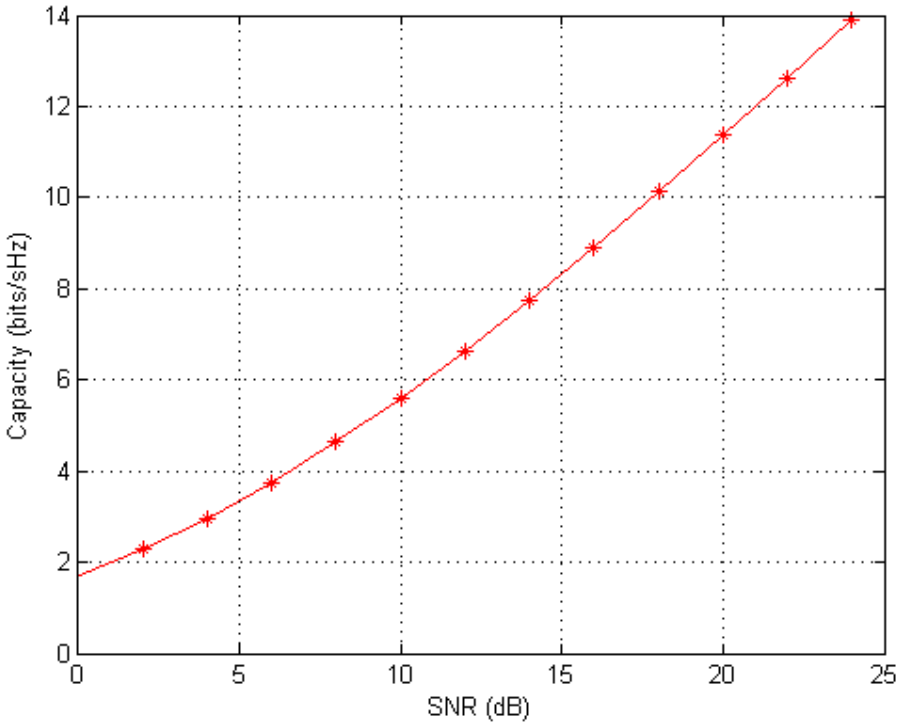

Figure 2.4. MIMO channel capacity for 2-tx and 2-rx antenna.

2.3.2.1 Capacity of a Deterministic MIMO Channel

The channel matrix is deterministic and its value *H is* known at the receiver. It can be shown that for a given realization of the channel **H** = *H*, the mutual information is maximized by a circularly symmetric complex Gaussian input codeword. Let us define K_c as the covariance of the input **C**. Then, the capacity is defined as the maximum of the mutual information between the input and output given a power constraint *P* on the total transmission power of the input, that is Tr(K_c) ≤ *P*, where Tr(K_c) is the trace of a matrix K_c. In what follows, we use the notation in (2.8) and the constraint Tr(K_c) ≤ *N*. The mutual information between input and output for the given realization is

$$I\,(\mathbf{C};\ \mathbf{r}|\mathbf{H}\ =\ H) =\ \log 2\left(\det\left[I_M + \left(\frac{\gamma}{N}\right) H^H . K_C . H\right]\right) \tag{2.9}$$

Then, the capacity is the maximum of the mutual information,

$$C = \max_{Tr(K_c)\leq N} \log_2\left(\det\left[I_M + \left(\frac{\gamma}{N}\right) H^H . K_C . H\right]\right) \quad \text{bits/(s Hz)} \tag{2.10}$$

Considering $K_c = I_N$, the equal power allocation capacity can be calculated in terms of the positive eigenvalues of the matrix $H^H \cdot H$. Let us define r as the rank of matrix H and λ_i , i = 1, 2, . . . , r as the non-zero eigenvalues of the matrix $H^H.H$. Then, the eigenvalues λ_i , i = 1, 2, . . . , r are positive real numbers above equation is written as

$$C = \max_{\sum_{i=1}^{r} \gamma_i = \gamma} \sum_{i=1}^{r} \log_2(1 + \gamma_i \lambda_i) \tag{2.11}$$

The above capacity is calculated using a water-filling algorithm [27]. Where an equal distribution of the power, $\gamma_i = \frac{\gamma}{N}$.

2.3.2.2 Capacity of a Random MIMO Channel

In this the channel matrix **H** is random in nature; the capacity in (2.10) is also a random variable. In general, when **H** is a memoryless channel based on the iid Rayleigh fading model, we can calculate the distribution of the capacity. For the case of $N \geq M$, one can derive a lower bound on the capacity in terms of chi-square random variables [22].

$$C > \sum_{k=N-M+1}^{N} \log_2\left(1 + \left(\frac{\gamma}{N}\right) . \chi_k\right) \tag{2.12}$$

where χ_k is a chi-square random variable with 2k degrees of freedom. The probability density function (pdf) of the chi-square random variable with 2k degrees of freedom is

$$f_{\chi_k}(x) = \frac{e^{-x} x^{k-1}}{[k-1]!} \quad , \qquad x > 0 \tag{2.13}$$

For the special case of $N = M$, we denote the lower bound in (2.12) by C_N

$$C_N = \sum_{k=1}^{N} \log_2\left(1 + \left(\frac{\gamma}{N}\right) . \chi_k\right) \tag{2.14}$$

This result suggests that for large N, the lower bound C_N increases at least linearly as a function of N [22], and indicates that when the number of transmit and receive antennas are the same, the capacity of a MIMO channel increases linearly by the number of antennas. In general, the capacity increases by the minimum of the number of transmit

and receive antennas. One can show that at high SNRs the capacity of a MIMO channel in (2.10) in terms of γ , the received SNR, can be described as

$$C \approx \min_{\{N,M\}} \log_2\left(\frac{\gamma}{N}\right) + \sum_{k=|N-M|+1}^{\min\{N,M\}} \log_2(\chi_k) \tag{2.15}$$

where χ_k is a chi-square random variable with 2*k* degrees of freedom.

2.4 Summary

In this chapter we studied background and model of wireless channel, its applications, and challenges and about its parameters. Also we discussed how to maintain wireless channel environment performance and its effects such as diversity and fading. A typical course on MIMO system model may start with some background material on wireless communications and capacity of MIMO channels as covered in this chapter.

Throughout the chapter, we provide different solutions to some of the challenges in wireless communication by using multiple antennas. The main topic of this book is how to overturn the difficulties in wireless communication by employing multiple antennas. We start with a study of the capacity increase due to the use of multiple antennas. Then, we show how to design space-time architecture for multiple transmit antennas to improve the performance of a wireless system while keeping the transmission power intact. Simulation result for MIMO capacity vs SNR with 2-tx and 2-rx antenna was also provided.

CHAPTER 3

SPACE TIME CODES

Space-time coding is a coding technique designed for use with multiple transmits antennas. Coding is performed in both spatial and temporal domains to introduce correlation between signals transmitted from various antennas at various time periods. The spatial-temporal correlation is used to exploit the MIMO channel fading and minimize transmission errors at the receiver. Space-time coding can achieve transmit diversity and power gain over spatially uncoded systems without sacrificing the bandwidth.

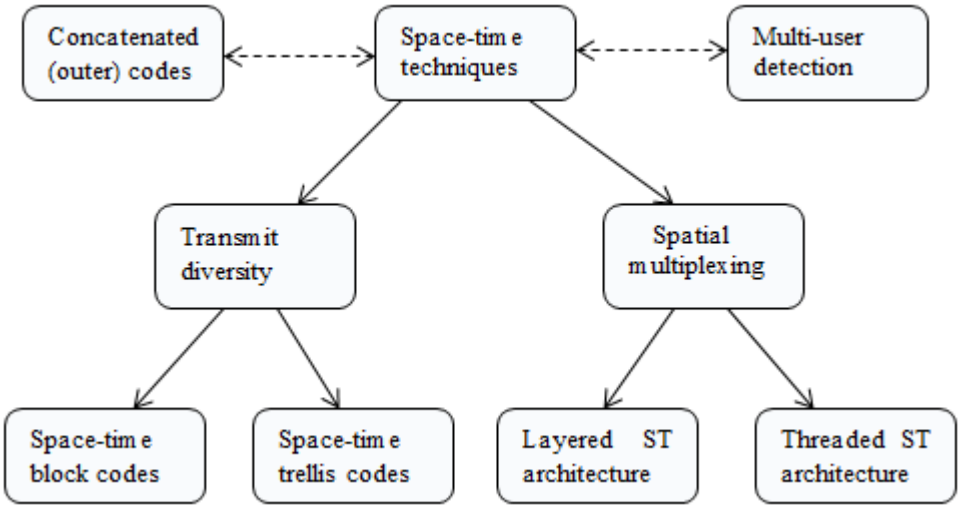

Figure 3.1. Classification of space-time coding techniques.

There are various approaches in coding structures, including space-time block codes (STBC), space-time trellis codes (STTC), space-time turbo trellis codes and layered space-time (LST) codes. Figure 3.1 illustrates the classification of space-time coding techniques and related areas of research. A central issue in all these schemes is the exploitation of multipath effects in order to achieve high spectral efficiencies and performance gains.

A good code follows a design criterion that adds some conception of optimality to the code. Figure 3.2 shows the block diagram of space-time coding system. In this, let us consider transmission over a binary symmetric channel using a linear binary block channel code. The bit error rate of the system depends on the Hamming distances of the

codeword pairs. Defining the set of all possible codeword pairs and the corresponding set of Hamming distances, we denote the minimum Hamming distance by d_{min}. It can be shown that a code with minimum Hamming distance d_{min} can correct all error patterns of weight less than or equal to $\lfloor (d_{min} - 1)/2 \rfloor$, where $\lfloor x \rfloor$ is the largest integer less than or equal to *x*. Therefore, for a given redundancy, a "good" code has a high minimum Hamming distance. The design criterion for such a code is to maximize the minimum possible Hamming distance among the codeword pairs. To compare two codes with similar redundancies, the one with higher Hamming distance is preferable. Similarly for an AWGN channel, a good design criterion is to maximize the minimum Euclidean distance among all possible codeword pairs.

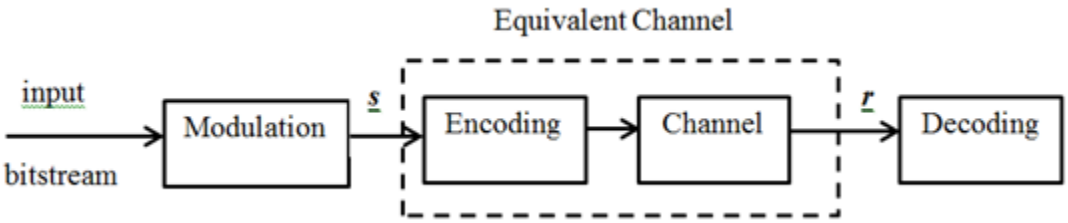

Figure 3.2. Block diagraam of space-time coding system.

We derive design criteria that guarantee the maximum possible diversity gain and coding gain at high SNRs. Also, we consider maximizing the mutual information between the input and output of the system as a design criterion.

3.1 Rank and Determinant Criteria

The rank & determinant criterion was the first criterion used for designing STCs, and was introduced by Tarokh [14] in 1998. The criterion is based on the rank and determinant of a matrix called as the *codeword difference matrix*. In order to come up with a design criterion, first we need to quantify the effects of mistaking two codewords with each other. In the case of a space-time code, a codeword is a $T \times N$ matrix given by (2.3). Let us assume that we transmit a codeword $\mathbf{C^1}$.

$$\mathbf{C}^1 = \begin{pmatrix} C_{1,1}^1 & C_{1,2}^1 & \cdots & C_{1,N}^1 \\ C_{2,1}^1 & C_{2,2}^1 & \cdots & C_{2,N}^1 \\ \vdots & \vdots & \ddots & \vdots \\ C_{T,1}^1 & C_{T,2}^1 & \cdots & C_{T,N}^1 \end{pmatrix} \tag{3.1}$$

An error occurs if the decoder mistakenly decides that we have transmitted another codeword, for example $\mathbf{C^2}$.

$$\mathbf{C}^2 = \begin{pmatrix} C_{1,1}^2 & C_{1,2}^2 & \cdots & C_{1,N}^2 \\ C_{2,1}^2 & C_{2,2}^2 & \cdots & C_{2,N}^2 \\ \vdots & \vdots & \ddots & \vdots \\ C_{T,1}^2 & C_{T,2}^2 & \cdots & C_{T,N}^2 \end{pmatrix} \tag{3.2}$$

If the codebook (the set of all codewords) only contains $\mathbf{C^1}$ and $\mathbf{C^2}$, we denote the pairwise error probability (PEP) [10] of transmitting $\mathbf{C^1}$ and detecting it as $\mathbf{C^2}$ by $P(\mathbf{C^1} \rightarrow \mathbf{C^2})$. Note that in general when the codebook contains I codewords, using the union bound, the probability of error when we transmit $\mathbf{C^1}$ is upper bounded by

$$P(\text{error}|\mathbf{C^1}\text{is sent}) \leq \sum_{i=2}^{I} P(\mathbf{C^1} \rightarrow \mathbf{C}^i) \tag{3.3}$$

The overall bound on error probability can be calculated by using (3.3). We calculate the PEP $P(\mathbf{C^1} \rightarrow \mathbf{C^2})$ and use it to define the design criteria. First we assume a fixed known channel matrix **H** and then calculate the average error by computing the expected value over the distribution of the **H**.

Without loss of generality, we use (2.6) to represent the input–output relationship of the channel and the corresponding normalization from Section 2.3.1. The average symbol transmission power from each antenna is $E_s = 1/N$ and the variance of a noise sample is $[|\eta_{t,m}|^2] = N_0 = 1/\gamma$. We consider the distribution of the received signals for a known codeword **C** and channel matrix **H**, that is $f(\mathbf{r}|\mathbf{C},\mathbf{H})$. Since $\mathcal{N}$ is Gaussian Random Variable (GRV) for fixed **C** and **H**, the received vector **r** is also a multivariate, multidimensional, GRV. Therefore,

$$f(\mathbf{r}|\mathbf{C},\mathbf{H}) = \frac{1}{(\pi N_0)^{\frac{M\text{x}M}{2}}} \exp\left\{\frac{-\text{Tr}[(\mathbf{r}-\mathbf{C}.\mathbf{H})^{\mathbf{H}}(\mathbf{r}-\mathbf{C}.\mathbf{H})]}{N_0}\right\}$$

$$= \left(\frac{\gamma}{\pi}\right)^{\frac{M\text{x}M}{2}} \exp\{-\gamma \text{Tr}[(\mathbf{r}-\mathbf{C}.\mathbf{H})^{\mathbf{H}}(\mathbf{r}-\mathbf{C}.\mathbf{H})]\} \tag{3.4}$$

The Frobenius norm of matrix A is denoted by $||A||_F$ and is defined as

$$||A||_F = \sqrt{Tr(A^H.A)} = \sqrt{Tr(A.A^H)} \tag{3.5}$$

One can rewrite (3.4) in terms of a Frobenius norm as follows:

$$f(\mathbf{r}|\mathbf{C},\mathbf{H}) = \left(\frac{\gamma}{\pi}\right)^{\frac{M\text{x}M}{2}} \exp\left\{-\gamma\left|\left|\mathbf{r}-\mathbf{C}.\mathbf{H}\right|\right|_{\mathrm{F}}^{2}\right\}$$

$$= \left(\frac{\gamma}{\pi}\right)^{\frac{M\text{x}M}{2}} \exp\left\{-\gamma\sum_{t=1}^{T}\sum_{m=1}^{M}\left|(\mathbf{r}-\mathbf{C}.\mathbf{H})_{t,m}\right|^{\mathbf{2}}\right\} \tag{3.6}$$

Where $\left|\left|\mathbf{r}-\mathbf{C}.\mathbf{H}\right|\right|_{\mathrm{F}}^{2} = \sum_{t=1}^{T}\sum_{m=1}^{M}\left|(\mathbf{r}-\mathbf{C}.\mathbf{H})_{t,m}\right|^{\mathbf{2}}$ is derived from the definition of the Frobenius norm in (3.5). Maximum-likelihood (ML) decoding decides in favor of a codeword that maximizes $f(\mathbf{r}|\mathbf{C},\mathbf{H})$. Let us assume that we transmit $\mathbf{C^1}$, the received vector is $\mathbf{r^1} = \mathbf{C^1}.\mathbf{H} + \mathbb{N}^{\mathbf{1}}$ and given the channel matrix $\mathbf{H}$, the pairwise error probability is calculated by

$$P(\mathbf{C^1} \to \mathbf{C^2}|\mathbf{H}) = P\left(\left\|\mathbf{r^1}-\mathbf{C^1}.\mathbf{H}\right\|_{\mathrm{F}}^{2} - \left\|\mathbf{r^1}-\mathbf{C^2}.\mathbf{H}\right\|_{\mathrm{F}}^{2} > 0|\mathbf{H}\right) \tag{3.7}$$

We rewrite (3.7) to calculate the pairwise error probability as follows:

$$P(\mathbf{C^1} \to \mathbf{C^2}|\mathbf{H}) = P\left\{\mathrm{Tr}\left([(\mathbf{C^1}-\mathbf{C^2}).\mathbf{H}+\mathbb{N}^{\mathbf{1}}]^H.[(\mathbf{C^1}-\mathbf{C^2}).\mathbf{H}+\mathbb{N}^{\mathbf{1}}] - \mathbb{N}^{\mathbf{1}^H}\mathbb{N}^{\mathbf{1}}\right) < 0|\mathbf{H}\right\}$$

$$= P(\mathrm{Tr}\{\mathbf{H}^H.(\mathbf{C^1}-\mathbf{C^2})^H.(\mathbf{C^1}-\mathbf{C^2}).\mathbf{H}\} - X < 0|\mathbf{H})$$

$$= P\left(\left\|(\mathbf{C^1}-\mathbf{C^2}).\mathbf{H}\right\|_F^2 < X|\mathbf{H}\right)$$

$$= P\left(X > \left\|(\mathbf{C^2}-\mathbf{C^1}).\mathbf{H}\right\|_F^2|\mathbf{H}\right) \tag{3.8}$$

where given $\mathbf{H}$, $X = \mathrm{Tr}\left\{\mathbb{N}^{\mathbf{1}^H}.(\mathbf{C^2}-\mathbf{C^1}).\mathbf{H} + \mathbf{H}^H.(\mathbf{C^2}-\mathbf{C^1})^H.\mathbb{N}^{\mathbf{1}}\right\}$ is a zero mean Gaussian random variable with variance $2N_0\left\|(\mathbf{C^2}-\mathbf{C^1}).\mathbf{H}\right\|_F^2 = (2/\gamma)\left\|(\mathbf{C^2}-\mathbf{C^1}).\mathbf{H}\right\|_F^2$. Therefore, one can calculate the pairwise error probability (PEP) using the Q function as

$$P(\mathbf{C^1} \to \mathbf{C^2}|\mathbf{H}) = Q\left(\frac{||(\mathbf{C^2}-\mathbf{C^1}).\mathbf{H}||_F^2}{\sqrt{\left(\frac{2}{\gamma}\right)||(\mathbf{C^2}-\mathbf{C^1}).\mathbf{H}||_F^2}}\right)$$

$$= Q\left(\sqrt{\frac{\gamma}{2}}||(\mathbf{C^2} - \mathbf{C^1}).\mathbf{H}||_F^2\right) \tag{3.9}$$

where

$$Q(x) = \frac{1}{\sqrt{2\pi}}\int_x^\infty e^{\frac{-y^2}{2}}dy \tag{3.10}$$

Therefore, it remains to calculate $||(\mathbf{C^2} - \mathbf{C^1}).\mathbf{H}||_F^2$ to derive the conditional pairwise error probability. Let us define the error (difference) matrix $\boldsymbol{D}(\mathbf{C^1}, \mathbf{C^2}) = \mathbf{C^2} - \mathbf{C^1}$. We write the PEP in terms of the eigenvalues of a matrix $\boldsymbol{A}(\mathbf{C^1}, \mathbf{C^2}) = \boldsymbol{D}(\mathbf{C^1}, \mathbf{C^2})^H.\boldsymbol{D}(\mathbf{C^1}, \mathbf{C^2}) = (\mathbf{C^2} - \mathbf{C^1})^H.(\mathbf{C^2} - \mathbf{C^1})$. Since $\boldsymbol{D}(\mathbf{C^1}, \mathbf{C^2})$ is a square root of $\boldsymbol{A}(\mathbf{C^1}, \mathbf{C^2})$, the eigenvalues of $\boldsymbol{A}(\mathbf{C^1}, \mathbf{C^2})$ denoted by λ_n, *n=1, 2, ..., N* are non-negative real numbers, $\lambda_n \geq 0$. Using the singular value decomposition theorem [40], we have

$$\boldsymbol{A}(\mathbf{C^1}, \mathbf{C^2}) = V^H.\ \wedge.V \tag{3.11}$$

Where $\wedge = diag(\lambda_1, \lambda_2, \ldots, \lambda_N)$. Therefore,

$$||(\mathbf{C^2} - \mathbf{C^1}).\mathbf{H}||_F^2 = \mathrm{Tr}[\mathbf{H}^H.\boldsymbol{A}(\mathbf{C^1}, \mathbf{C^2}).\mathbf{H}]$$

$$= \mathrm{Tr}[\mathbf{H}^H.V^{\boldsymbol{H}}.\wedge.V.\mathbf{H}] \tag{3.12}$$

Since the elements of **H** are independent Gaussian random variables, the elements of $V \cdot \mathbf{H}$ are also Gaussian. We denote the $(n,m)^{th}$ element of $V \cdot \mathbf{H}$ by $\beta_{n,m}$. Therefore,

$$||(\mathbf{C^2} - \mathbf{C^1}).\mathbf{H}||_F^2$$

$$= \mathrm{Tr}\left[\begin{pmatrix} \beta_{1,1}^* & \beta_{2,1}^* & \cdots & \beta_{N,1}^* \\ \beta_{1,2}^* & \beta_{2,2}^* & \ldots & \beta_{N,2}^* \\ \vdots & \vdots & \ddots & \vdots \\ \beta_{1,M}^* & \beta_{2,M}^* & \cdots & \beta_{N,M}^* \end{pmatrix} \cdot \begin{pmatrix} \lambda_1 & 0 & \cdots & 0 \\ 0 & \lambda_2 & \ldots & 0 \\ \vdots & \vdots & \ddots & \vdots \\ 0 & 0 & \cdots & \lambda_N \end{pmatrix} \cdot \begin{pmatrix} \beta_{1,1} & \beta_{1,2} & \cdots & \beta_{1,,M} \\ \beta_{2,1} & \beta_{2,2} & \ldots & \beta_{2,M} \\ \vdots & \vdots & \ddots & \vdots \\ \beta_{N,1} & \beta_{N,2} & \cdots & \beta_{N,M} \end{pmatrix}\right]$$

$$= \mathrm{Tr}\left[\begin{pmatrix} \sum_{n=1}^{N} \lambda_n \left|\beta_{n,1}\right|^2 & \cdots & \ldots \\ \vdots & \sum_{n=1}^{N} \lambda_n \left|\beta_{n,2}\right|^2 & \vdots \\ \ldots & \cdots & \sum_{n=1}^{N} \lambda_n \left|\beta_{n,M}\right|^2 \end{pmatrix}\right] \tag{3.13}$$

$$= \sum_{m=1}^{M} \sum_{n=1}^{N} \lambda_n \left|\beta_{n,m}\right|^2 \tag{3.14}$$

Putting (3.14) in (3.9) we get,

$$P(\mathbf{C^1} \rightarrow \mathbf{C^2}|\mathbf{H}) = Q\left(\sqrt{\frac{\gamma}{2} \sum_{m=1}^{M} \sum_{n=1}^{N} \lambda_n \left|\beta_{n,m}\right|^2}\right) \tag{3.15}$$

A good upper bound on the Q function is $Q(x) \leq \frac{1}{2} e^{\frac{-x^2}{2}}$. Therefore, we can calculate an upper bound on the conditional PEP as follows:

$$P(\mathbf{C^1} \rightarrow \mathbf{C^2}|\mathbf{H}) \leq \frac{1}{2} \exp\left(-\frac{\gamma}{4} \sum_{m=1}^{M} \sum_{n=1}^{N} \lambda_n \left|\beta_{n,m}\right|^2\right) \tag{3.16}$$

Since $\beta_{n,m}$ are Gaussian, their magnitudes, $\left|\beta_{n,m}\right|$ are Rayleigh with the probability density function (pdf)

$$f\left(\left|\beta_{n,m}\right|\right) = 2\left|\beta_{n,m}\right| \exp\left(-\left|\beta_{n,m}\right|^2\right) \tag{3.17}$$

Using the distributions of $\left|\beta_{n,m}\right|$, we can calculate the expected value of the PEP,

$$P(\mathbf{C^1} \rightarrow \mathbf{C^2}) = E[P(\mathbf{C^1} \rightarrow \mathbf{C^2}|\mathbf{H}) \leq \frac{1}{\prod_{n=1}^{N} \left(1 + \frac{\gamma \lambda_n}{4}\right)^M} \tag{3.18}$$

If $\mathbf{A}(\mathbf{C^1} \rightarrow \mathbf{C^2})$ is full rank, none of its eigenvalues is zero. On the other hand, if its rank is $r<N$, without loss of generality, we have $\lambda_1 \geq \lambda_2 \geq \cdots \geq \lambda_r > 0$ and $\lambda_{r+1} = \cdots =$

$\lambda_N = 0$. At high SNRs, one can neglect the one in the denominator of the inequality (3.18) and write the following upper bound based on the nonzero eigenvalues:

$$P(\mathbf{C^1} \rightarrow \mathbf{C^2}) \leq \frac{4^{rM}}{(\prod_{n=1}^{r} \lambda_n)^M \, (\gamma)^{rM}} \tag{3.19}$$

Without loss of generality, let us assume that the worst case is transmitting $\mathbf{C^1}$ and decoding it as $\mathbf{C^2}$. We can define the diversity gain G_d and the coding gain G_c using right-hand side of (3.19). Using $(G_c\gamma)^{-G_d}$ to represent the right-hand side of (3.19), the diversity of the code is equal to *rM*. In other words, the diversity is equal to the rank of matrix $\boldsymbol{A}(\mathbf{C^1}, \mathbf{C^2})$ or equivalently the rank of the difference matrix $\boldsymbol{D}(\mathbf{C^1}, \mathbf{C^2})$ multiplied by the number of receive antennas. Similarly, the coding gain relates to the product of the nonzero eigenvalues of the matrix $\boldsymbol{A}(\mathbf{C^1}, \mathbf{C^2})$. A full diversity of *MN* is possible if the matrix $\boldsymbol{A}(\mathbf{C^1}, \mathbf{C^2})$ is full rank. In this case, the coding gain relates to the products of eigenvalues $\prod_{n=1}^{N} \lambda_n$ or equivalently the determinant of matrix $\boldsymbol{A}(\mathbf{C^1}, \mathbf{C^2})$. The coding gain distance (CGD) between codewords $\mathbf{C^1}$ and $\mathbf{C^2}$ is defined as CGD$(\mathbf{C^1}, \mathbf{C^2}) =$ det$\left(\boldsymbol{A}(\mathbf{C^1}, \mathbf{C^2}) \right)$. Therefore, a good design criterion to guarantee full diversity is to make sure that for all possible codewords $\mathbf{C}^i$ and $\mathbf{C}^j$ $i \neq j$, the matrix $\boldsymbol{A}\left(\mathbf{C}^i, \mathbf{C}^j\right)$ is full rank [14] [41]. Then, to increase the coding gain for a full diversity code, an additional good design criterion is to maximize the minimum determinant of matrices $\boldsymbol{A}\left(\mathbf{C}^i, \mathbf{C}^j\right)$ for all $i \neq j$. Thus, the rank criterion suggests that the error matrix $\boldsymbol{D}\left(\mathbf{C}^i, \mathbf{C}^j\right) = \mathbf{C}^j - \mathbf{C}^i$ has to be full rank for all $i \neq j$ in order to obtain full diversity *NM*. The determinant criterion says that the minimum determinant of $\boldsymbol{A}\left(\mathbf{C}^i, \mathbf{C}^j\right) = \boldsymbol{D}\left(\mathbf{C}^i, \mathbf{C}^j\right)^H \boldsymbol{D}\left(\mathbf{C}^i, \mathbf{C}^j\right)$ among all $i \neq j$ has to be large to obtain high coding gains.

3.2 Trace Criteria

In this criteria, first we recalculate (3.9) by rearranging the norm $||(\mathbf{C^2} - \mathbf{C^1}) \, . \mathbf{H}||_F$ as follows

$$||(\mathbf{C^2} - \mathbf{C^1}) \, . \mathbf{H}||_F^2 = \mathrm{Tr}[\boldsymbol{D}(\mathbf{C^1}, \mathbf{C^2}). \boldsymbol{H}. \{\boldsymbol{D}(\mathbf{C^1}, \mathbf{C^2}). \boldsymbol{H}\}^H] \tag{3.20}$$

We calculate the expected value of (3.20) over the distribution of the channel matrix. Since the elements of **H** are independent Gaussian random variables, we have

$$E[\boldsymbol{H}.\mathbf{H}^H] = MI_N \tag{3.21}$$

where I_N is the $N \times N$ identity matrix. Therefore, we can calculate

$$\begin{aligned} E||(\mathbf{C^2} - \mathbf{C^1}).\mathbf{H}||_F^2 &= M\ \mathrm{Tr}[\boldsymbol{D}(\mathbf{C^1},\mathbf{C^2}).\boldsymbol{D}(\mathbf{C^1},\mathbf{C^2})^H] \\ &= M\ \mathrm{Tr}[\boldsymbol{A}(\mathbf{C^1},\mathbf{C^2})] \\ &= M||\boldsymbol{D}(\mathbf{C^1},\mathbf{C^2})||_F^2 \end{aligned} \tag{3.22}$$

Since $\boldsymbol{D}||(\mathbf{C^1},\mathbf{C^2})||_F$ is a metric on the codebook of the space-time code. In other words,

(i) it is symmetric $\boldsymbol{D}||(\mathbf{C^1},\mathbf{C^2})||_F = \boldsymbol{D}||(\mathbf{C^2},\mathbf{C^1})||_F$

(ii) it is zero if and only if $\mathbf{C^1} = \mathbf{C^2}$

(iii) the triangle inequality $\boldsymbol{D}||(\mathbf{C^2},\mathbf{C^1})||_F \leq \boldsymbol{D}||(\mathbf{C^1},\mathbf{C^3})||_F + \boldsymbol{D}||(\mathbf{C^3},\mathbf{C^2})||_F$ holds.

Therefore, it can be used as a distance measure between space-time codewords. This distance measure is of course independent of the channel matrix.

Another approach to further study the behaviors of the norm $||(\mathbf{C^2} - \mathbf{C^1}).\mathbf{H}||_F$ is to consider a large number of receive antennas [29] using upper bound as in (3.16) the PEP is

$$P(\mathbf{C^1} \rightarrow \mathbf{C^2}) \leq \frac{1}{2}\exp\left(-M||\boldsymbol{D}(\mathbf{C^1},\mathbf{C^2})||_F^2\frac{\gamma}{4}\right) \tag{3.23}$$

Another approach to derive a similar bound is to use the central limit theorem to calculate the norm in (3.14) [17]. The distribution of $|\beta_{n,m}|^2$ is chi-square with unit mean and variance for all values of *n* and *m*. Thus PEP is [17]

$$P(\mathbf{C^1} \rightarrow \mathbf{C^2}) \leq \frac{1}{4}\exp\left(-M||\boldsymbol{D}(\mathbf{C^1},\mathbf{C^2})||_F^2\frac{\gamma}{4}\right) \tag{3.24}$$

As can be seen from bounds (3.23) and (3.24), the PEP is related to the metric $\boldsymbol{D}||(\mathbf{C^1},\mathbf{C^2})||_F$. It is argued in [42] and [29] that a good design criterion is to maximize the minimum distance $\boldsymbol{D}||(\mathbf{C^i},\mathbf{C^j})||_F$ among all possible $i \neq j$. This is called "trace criterion" because $\boldsymbol{D}||(\mathbf{C^1},\mathbf{C^2})||_F^2 = \mathrm{Tr}[\boldsymbol{A}(\mathbf{C^1},\mathbf{C^2})]$. As shown above, a good property of

such a design criterion is that $\boldsymbol{D}||(\mathbf{C^1}, \mathbf{C^2})||_F$ is a metric on the codebook of the space-time code. Therefore, it provides all the good properties of a distance measure.

3.3 Maximum Mutual Information Criteria

This criterion selects the code parameters to maximize the mutual information between the transmitted and received signals. Let us denote the vector of data symbols by *s*. The codeword **C** is defined as a function of the symbol vector *s* using the structure of the code. As shown in Figure 3.1, the combination effect of the encoder and the channel on the data symbols can be considered as an "equivalent channel" $\boldsymbol{H}$. Then, the input–output relationship between the data symbols and the received signals *r* is

$$r = s.\boldsymbol{H} + \boldsymbol{N} \tag{3.25}$$

where $\boldsymbol{N}$ is the additive Gaussian noise of the channel. The goal is to design the code such that the mutual information between input *s* and output *r* is maximized. Such a design criterion is mostly beneficial to maximize the throughput spatial multiplexing gain. Such a design criterion is that for the goal of maximizing the throughput, the code should not limit the capacity of the MIMO channel. Therefore, the "best" code is the one for which the mutual information between input *s* and output *r* is equal to the capacity of the original channel. Of course, like any other capacity argument, such an optimization is subjected to some power constraints on the input. The maximum mutual information criterion does not provide a unique design for a given structure.

3.4 Summary of Space –Time Coding

Much of the existing work in space-time coding concentrates on slow or quasi-static, flat, and spatially independent fading channels. These assumptions are relevant to narrowband communications with low mobility in rich scattering environments. However, they are not representative of the channels applicable to broadband wireless access, a technology that we believe will become increasingly important in years to come. The broadband wireless access channel is a slow, frequency selective fading channel, which may experience medium to high spatial correlation, depending on the applications being considered. Although spatial correlation reduces the achievable capacity, its frequency selectivity provides additional diversity which can be exploited to improve the performance of a system communicating over this channel.

In the beginning of this chapter we studied the classification of space-time coding techniques and related areas of research. A central issue in all these schemes is the exploitation of multipath effects in order to achieve high spectral efficiencies and performance gains.

We derive design criteria that guarantee the maximum possible diversity gain and coding gain at high SNRs. In section 3.1, 3.2 and 3.3 we derived mathematical expression for rank and determinant criteria (RDC), trace criteria (TC) and maximum mutual information criteria respectively. The RDC criteria is suitable for $rn_R < 4$, otherwise TC criteria is suitable.

CHAPTER 4

SPACE TIME TRELLIS CODES

Introduction

Space-time trellis codes (STTCs) combine modulation and trellises coding to transmit information over multiple transmit antennas and MIMO channels. The goal is to construct trellis codes satisfying the space-time coding design criteria. To achieve full diversity, a STTC should satisfy the rank criterion as discussed in Chapter 3. Of course among all possible full-rate, full-diversity codes, the one that provides the highest coding gain is preferable. The first example of a rate one full diversity space-time trellis code is the delay diversity scheme in [23]. Let us assume a constellation that maps *b* bits of data to a symbol. The delay diversity scheme uses every *b* input bit to pick one symbol that is transmitted from the first antenna. Then, the second antenna transmits the same symbols with a delay of one symbol. Maximum-likelihood decoding is used at the receiver to recover the transmitted symbols. Since the symbols go through two independent channel path gains, a diversity of two is achieved for one receive antenna (or per receive antenna). Delay diversity is a special case of STTCs presented in [14]. Different examples of STTCs for BPSK, QPSK, 8-PSK, and 16-QAM constellations are designed in [14]. In some cases, the proposed STTCs in [14] are delay diversity codes. In other cases, they provide a higher coding gain and better performance compared to the delay diversity codes.

In this Chapter a brief description of a STTC based wireless system is given in Section 4.1. Then in Section 4.2 we discuss STTC construction. We give a simple example to illustrate this construction. In Section 4.3 we provide a discussion of the performance criteria. We present a basis for STTC performance over Rayleigh, Rician and Nakagami fading channels. In Section 4.4 we present some STTC codes given in the literature. A brief description of channel estimation and STTC decoding is presented in Section 4.5. In Section 4.6 performance evaluations were carried out for STTC based MIMO fading channels such as Rayleigh, Rician and Nakagami fading channels and comparison performed using simulation. We gave a summary of this Chapter in Section 4.7.

4.1 System Model of STTC Based Wireless System

A typical STTC based wireless system has an encoder, pulse shaper, modulator and multiple transmit antennas at the transmitter, and the receiver has one or more receive antennas, demodulator, channel estimator and STTC decoder. We consider a mobile communication system with n_T transmit antennas and n_R receive antennas as shown in figures 4.1 (a) and (b). The space-time trellis encoder encodes the data *s(t)* coming from the information source and Space Time Trellis Encoder encodes the data which is divided by performing serial to parallel conversion into n_T streams of data as $c_t^1, c_t^2, \dots, c_t^{n_t}$. Each of these streams of data passes through a pulse shaper before being modulated. The output of modulator i at time slot t is the signal c_t^i, which transmitted through transmit antenna i. Here $1 \leq i \leq n_T$. The transmitted symbols have symbol energy of E_s. We assume that the n_t signals are transmitted simultaneously from the antennas having transmission period T as shown in figure 4.1 (a). In the receiver, each antenna receives a superposition of n_t transmitted signals corrupted by noise and multipath fading and then the received signal is demodulated and decoded by estimating channel response. Here Space Time Trellis Decoder must have the knowledge of CSI to estimate the channel response. Let the complex channel coefficient between transmit antenna i and receive antenna j have a value of $h_{i,j}(t)$ at time t, where$1 \leq i \leq n_R$.

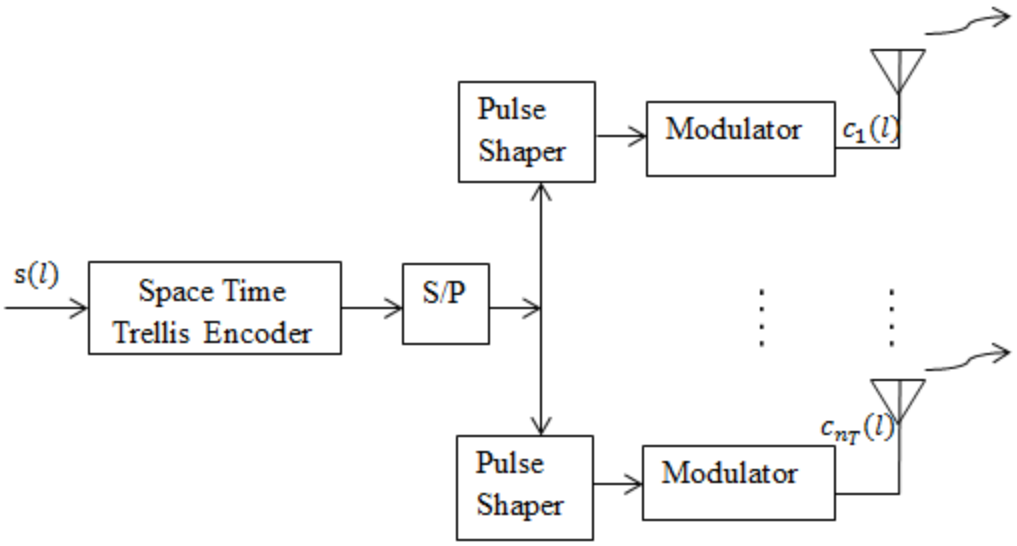

(a)

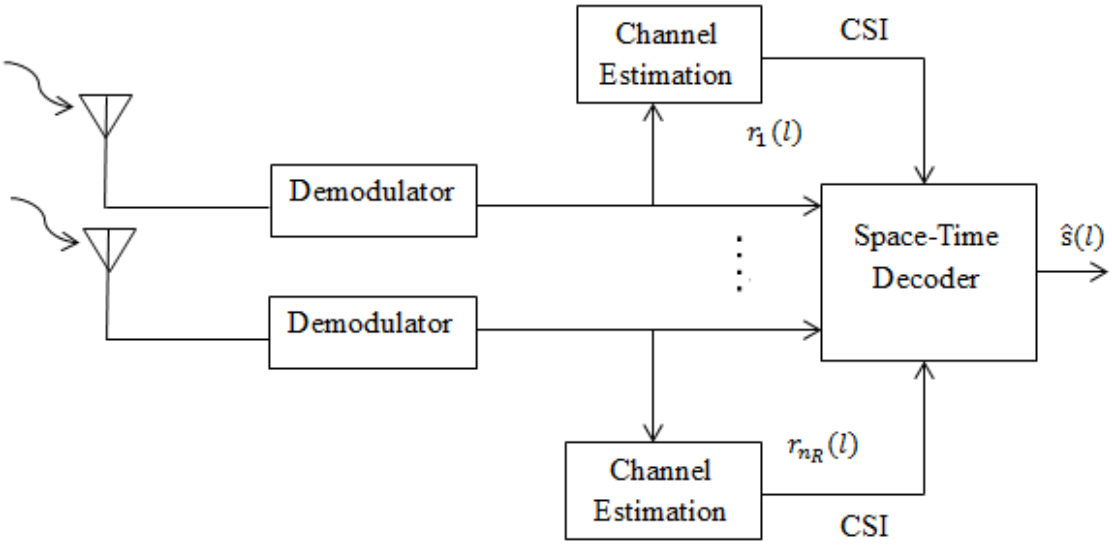

(b)

Figure 4.1. A block diagram of the (a) transmitter and (b) receiver of a STTC based system.

Thus received signal at antenna j, j= 1, 2, ...,n_R [14] is then

$$r_t^j = \sqrt{E_s}\sum_{i=1}^{n} h_{i,j}(t)c_t^j(t) + n_t^j \tag{4.1}$$

Where n_t^j the additive white Gaussian noise (AWGN) at is receive antenna j, which has zero mean and power spectral density N_0. We assume the channel coefficients $h_{i,j}(t)$ are modelled as samples of independent complex Gaussian random variables variance 0.5 per dimension [17].

4.2 Construction of Codes

STTCs are represented in a number of ways, such as the trellis form or generator matrix form as illustrated in figure 4.2 for a simple STTC. In [24], most codes are presented in trellis form. But for a systematic code search, the generator matrix form is preferable. The generator matrix representation is also used for convolutional codes [11], [12] and [25]. However the generator matrix notation as shown in figure 4.2 (b) is a little different than that used for convolutional codes [16]. In figure 4.2 (b) two input bits I_t^1 and I_t^2 enters the encoder at every time of symbol period. The input streams and its delayed versions are

multiplied by the branch coefficients or generator coefficients (a_0^1, a_0^2) and (a_1^1, a_1^2) respectively to I_t^1 and (b_0^1, b_0^2) and (b_1^1, b_1^2) to I_t^2 . The output of generator combines these input streams as (x_t^1, x_t^2). According to trellis diagram of figure 4.2 (a) the generator description is described as shown in figure 4.2 (b) and its coefficients can be put into a matrix form which is known as generator matrix. The generator matrix for 4-state is then given by

$$G = \begin{bmatrix} a_0^1 & b_0^1 & a_1^1 & b_1^1 \\ a_0^2 & b_0^2 & a_1^2 & b_1^2 \end{bmatrix}$$

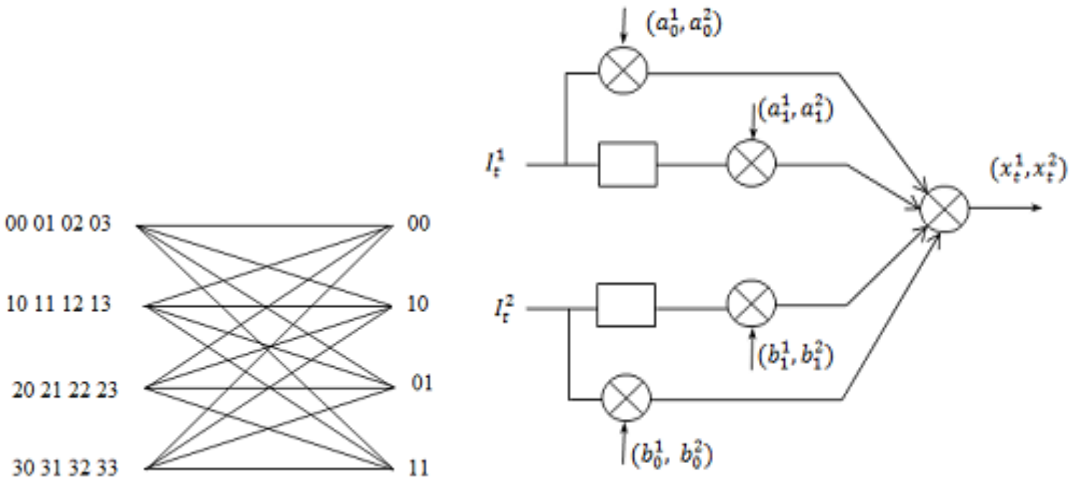

(a) (b)

Figure 4.2. (a) Trellis diagram and (b) generator matrix description of a STTC.

The following example illustrates STTC encoding. In Figure 4.3 we provide a trellis diagram and a table of output symbols related to the input bits and current state. This trellis is for 4-PSK constellations. Let the input symbol stream to the encoder is [2 3 2 1 0 1….]. Initially the encoder is in state "0". Thus "0" will be transmitted from the first antenna, the second antenna transmits "2" and the encoder goes into state "2" [26]. In this way for this input symbol stream the output for the 4-PSK STTC is as follows

$$c = \begin{bmatrix} 0 & 2 & 3 & 1 & 0 & 1 \\ 2 & 3 & 1 & 0 & 1 & \dots \end{bmatrix}$$

State	Output Symbols			
	Input 0	Input 1	Input 2	Input 3
0	00	01	02	03
1	10	11	12	13
2	20	21	22	23
3	30	31	32	33

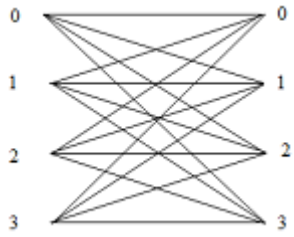

Figure 4.3. 4-PSK, 4-state STTC.

4.2.1 Code Construction of 4-State 4-PSK STTC

A signal constellation diagram for 4-PSK is shown in Figure 4.4 with 4-PSK information is contained in the signal phase. For 4-PSK, the phase takes one of four equally spaced values, such as 0, 2π/4, 4π/4 and 6π/4. These are typically represented by a Gray Code [25] and [27], as shown on the right side of Figure 4.4. These signal points are also labelled as 0, 1, 2 and 3. We can also express these in complex notation.

The encoder structure of a 4-state 4-PSK STTC is shown in Figure 4.2 (b), with bits input to the upper and lower branches. The memory orders of the upper and lower branches are υ_1 and υ_2, respectively. These are basically shift registers. The main purpose of the shift registers in the encoder is to store the previous transmitted bits. The length of the shift register is the memory of the encoder. The branch coefficients are arranged alternatively in the generator matrix, with representing the most significant bit (MSB). The input bit streams I_t^1 and I_t^2 are fed into the branches of the encoder with I_t^1 being the MSB. The output of the encoder is [14] [17]

$$x_t^k = \left(\sum_{p=0}^{\upsilon 1} I_{t-p}^1 \, a_p^k + \sum_{q=0}^{\upsilon 2} I_{t-q}^2 . b_{t-q}^k \right) \quad \text{mod } 4 \quad k = 1, 2 \tag{4.2}$$

where υ_1 and υ_2 the number of states is 2^v. v_i is calculated as

$$v_i = \left\lfloor \frac{v + i - 1}{2} \right\rfloor \qquad , \mathrm{i} = 1, 2 \tag{4.3}$$

Here $\lfloor x \rfloor$ denotes the largest integer smaller than or equal to *x*. For each branch, the output is the sum of the current input scaled by a coefficient and the previous input scaled by another coefficient. The two streams of input bits are passed through their respective shift register branches and multiplied by the coefficient pairs $\left(a_p^1, a_p^2\right)$ and $\left(\mathrm{b}_\mathrm{q}^1, b_q^2\right)$. Here

$$a_p^k, b_q^k \epsilon \{0, 1, 2, 3\}, \qquad k = 1, 2, p = 0, 1, \ldots, v_2$$

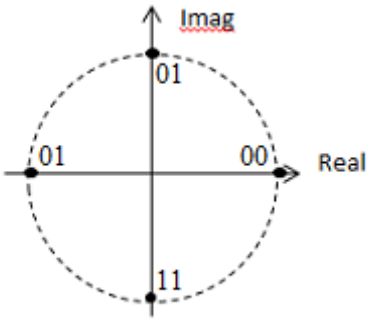

$0 \rightarrow 00 \Leftrightarrow 1 + 0j$

$1 \rightarrow 01 \Leftrightarrow 0 + 1j$

$2 \rightarrow 10 \Leftrightarrow -1 + 0j$

$3 \rightarrow 11 \Leftrightarrow 0 - 1j$

Figure 4.4. 4-PSK signal constellation diagram.

Then x_t^1 and x_t^2 are transmitted simultaneous through the first and second transmit antennas, respectively. Figures 4.5 (a) and (b) shows 8-state and 16 -state trellis diagrams respectively, for a rate of 2 b/s/Hz [24].

4.2.2 Code Construction of 8-State 8 PSK STTC

The 8 PSK, 8-state signal state constellation is shown in Figures 4.6. The trellis diagram and encoder structure of the 8-state 8 PSK trellis code is shown in Figure 4.7 which is very similar to Figure 4.2 except that it has three input antennas and three sets of coefficients. The additional input I_t^3 corresponds to a branch of memory order v_3. The total memory order is $v = v_1 + v_2 + v_3$. Here

$$v_i = \left\lfloor \frac{v + i - 1}{3} \right\rfloor \qquad , \mathrm{i} = 1, 2, 3 \tag{4.4}$$

The coefficient pairs are $(a_p^1, a_p^2), (b_q^1, b_q^2)and(c_s^1, c_s^2)$ for the input streams I_t^1, I_t^2 and I_t^3 respectively. The encoder output is

$$x_t^k = \left(\sum_{p=0}^{\upsilon 1} I_{t-p}^1 \, a_p^k + \sum_{q=0}^{\upsilon 2} I_{t-q}^2 \, b_{t-q}^k + \sum_{s=0}^{\upsilon 3} I_{t-s}^3 b_{t-s}^k \right) \mod 8 \text{ and } k = 1, 2 \tag{4.5}$$

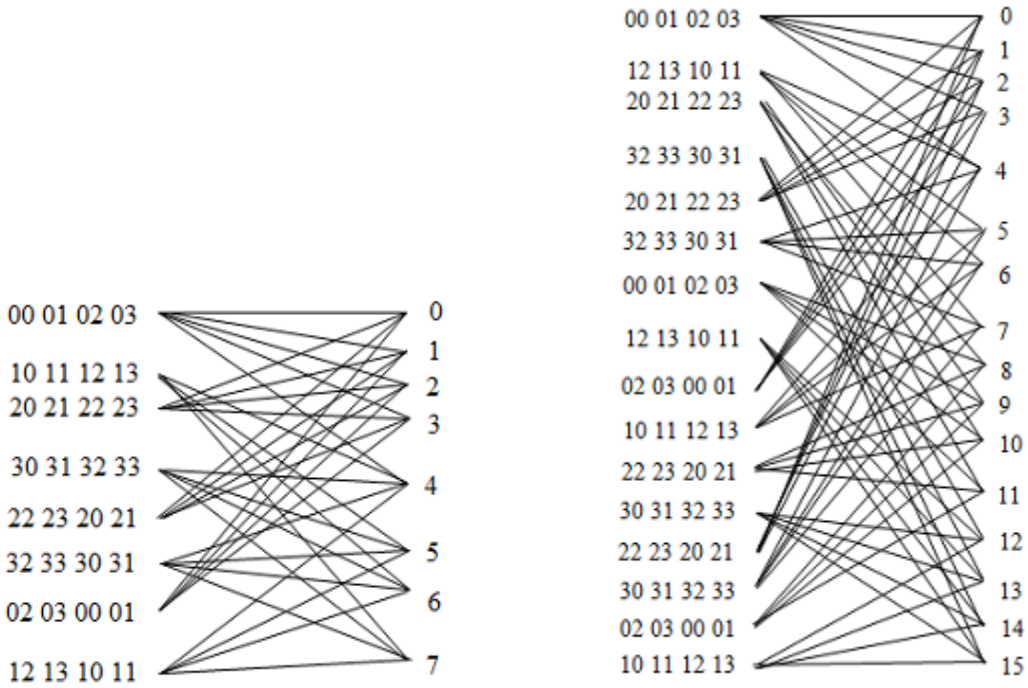

(a) (b)

Figure 4.5. (a) Trellis diagram of 4 PSK 8-state STTC.

(b) Trellis diagram of 4 PSK 16-state STTC.

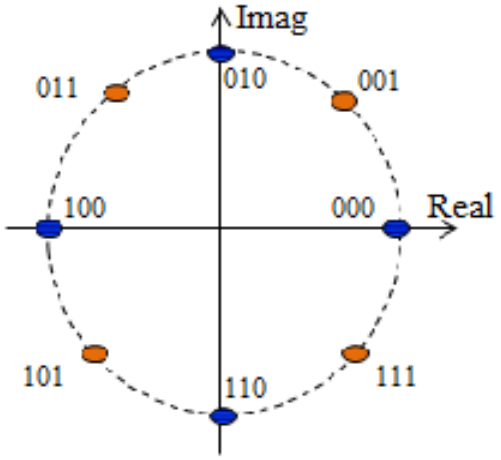

$$0 \rightarrow 000 \Leftrightarrow 1 + 0j$$

$$1 \rightarrow 001 \Leftrightarrow \frac{\sqrt{2}}{2} + \frac{\sqrt{2}}{2}j$$

$$2 \rightarrow 010 \Leftrightarrow 0 + 1j$$

$$3 \rightarrow 011 \Leftrightarrow -\frac{\sqrt{2}}{2} + \frac{\sqrt{2}}{2}j$$

$$4 \rightarrow 100 \Leftrightarrow -1 + 0j$$

$$5 \rightarrow 101 \Leftrightarrow -\frac{\sqrt{2}}{2} - \frac{\sqrt{2}}{2}j$$

$$6 \rightarrow 110 \Leftrightarrow 0 - 1j$$

$$7 \rightarrow 111 \Leftrightarrow \frac{\sqrt{2}}{2} - \frac{\sqrt{2}}{2}j$$

Figure 4.6. 8-PSK Signal constellation.

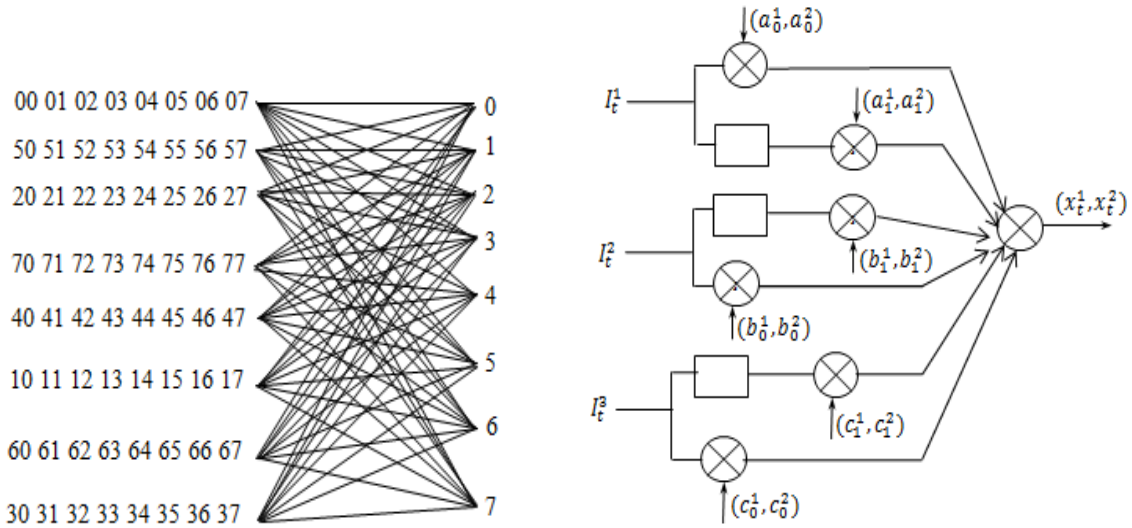

(a) (b)

Figure 4.7. (a) Trellis diagram and (b) encoder structure of an 8-PSK 8-state STTC.

4.3 Performance Criteria

We assume that the STTC codeword is given by [14]

$$c = \left(c_1^1 c_1^2 \ldots\ldots c_1^{n_T} c_2^1 c_2^2 \ldots\ldots c_2^{n_T} \ldots\ldots c_l^1 c_l^2 \ldots\ldots c_l^{n_T}\right) \tag{4.6}$$

Where l is the frame length. We consider a maximum likelihood receiver [31], which may possibly decide on an erroneous code word *e*, given by

$$e = \left(e_1^1 e_1^2 \ldots\ldots e_1^{n_T} e_2^1 e_2^2 \ldots\ldots e_2^{n_T} \ldots\ldots e_l^1 e_l^2 \ldots\ldots e_l^{n_T}\right) \tag{4.7}$$

We can write the difference code matrix, the difference between the erroneous codeword and the transmitted codeword as follows –

$$B(c,e) = \begin{bmatrix} e_1^1 - c_1^1 & e_2^1 - c_2^1 & \ldots & \ldots & e_l^1 - c_l^1 \\ e_1^2 - c_1^2 & e_2^2 - c_2^2 & \ldots & \ldots & e_l^2 - c_l^2 \\ \vdots & \vdots & \ddots & \ddots & \vdots \\ e_1^{n_T} - c_1^{n_T} & e_2^{n_T} - c_2^{n_T} & \cdots & \cdots & e_l^{n_T} - c_l^{n_T} \end{bmatrix} \tag{4.8}$$

The difference matrix *B(c, e)* has dimension n_T x l. From [24] we know that to achieve the maximum diversity order $n_R.n_T$ matrix *B(c, e)* must have full rank for all possible codewords *c* and *e*. If *B(c, e)* has minimum rank *r* over the set of pairs of distinct codewords then the diversity will be $r.n_R$ [24].

Let *A(c, e)= B(c, e) B*(c, e)* be the distance matrix, where *B*(c, e)* is the Hermitian of *B(c, e)*. The rank of *A(c, e)* is *r*. *A* has minimum dimension $n_T - r$ and exactly $n_T - r$ eigenvalues of *A are* zero. The non-zero eigenvalues of A are denoted by $\lambda_1, \lambda_2, \lambda_3, \ldots., \lambda_n$. Assuming perfect channel state information (CSI), the probability of transmitting *c* and deciding on an erroneous codeword *e* at the decoder is given by [14] [24] [17].

$$P\left(c, e\middle|h_{i,j}\right) = Q\left(\sqrt{\frac{E_s}{2N_0} d^2(c,e)}\right) \quad ;\ i = 1,2, \ldots., n_T, j = 1, 2, \ldots., n_R \tag{4.9}$$

$$\text{or,} \quad P(c \to e|h_{i,j}) \leq \exp\left(-\frac{d^2(c,e)E_s}{4N_0}\right) \tag{4.10}$$

where $N_0/2$ is the noise variance per dimension and

$$d^2(c,e) = \sum_{j=1}^{n_R} \sum_{t=1}^{l} \left| \sum_{i=1}^{n_T} h_{i,j}\left(c_t^i - e_t^i\right) \right|^2 \tag{4.11}$$

is the Euclidean distance. For independent Rician fading we can write (4.11) as [14].

$$P(c \to e) \leq \prod_{j=1}^{n_R} \left(\prod_{i=1}^{n_T} \frac{1}{1 + \frac{E_s}{4N_0}\lambda_i} \exp\left(- \frac{K_{i,j} \frac{E_s}{4N_0} \lambda_i}{1 + \frac{E_s}{4N_0}\lambda_i} \right) \right) \tag{4.12}$$

Here $K_{i,j}$ is a coefficient (Rician fading factor) and it is described in details in [14].

For the special case of Rayleigh fading we can assume $K_{i,j}$= 0 for all i and j [14]. Then (4.12) can be written as

$$P(c \to e) \leq \left(\frac{1}{\prod_{i=1}^{n_T} \left(1 + \frac{E_s}{4N_0}\lambda_i\right)} \right)^{n_R} \tag{4.13}$$

Let r denote the rank of matrix *A(c, e)*. The matrix *A* has dimension $n_T - r$ and $n_T - r$ eigenvalues of *A* are zero.

$$P(c \to e) \leq \left(\prod_{i=1}^{r} \lambda_i \right)^{-n_R} \left(\frac{E_s}{4N_0} \right)^{-r n_R} \tag{4.14}$$

We can derive following Design criteria for the STTC to achieve the best performance of a given system [14].

4.3.1 Design Criteria for STTC over Rayleigh Fading

4.3.1.1 Rank Criterion

The rank criterion optimizes the spatial diversity gain achieved by a STTC. Assume *B(c,e)* has minimum rank r over the set of pairs of distinct codewords so a diversity of r. n_R is achieved [14]. To illustrate this criterion [28], consider a 4-PSK system where the transmitted codeword is c=220313, and the erroneous codeword the receiver decides upon is e=330122. Figure 2.4 gives the 4-PSK signal constellation. In this example, n_T = 2 and the message length is L = 3. The 2 x 3 difference matrix is

$$B(c,e) = \begin{vmatrix} -j-(-1) & 1-1 & -1-j \\ -j-(-1) & j-(-j) & -1-(-j) \end{vmatrix}$$

$$= \begin{vmatrix} 1-j & 0 & -1-j \\ 1-j & 2j & j-1 \end{vmatrix}$$

The rank of *B(c, e)* is 2, as is the rank of *A(c, e)*. For this system with n_T = 2 transmit antennas and n_R = 1 receive antenna, the diversity gain is 2.

4.3.1.2 Determinant Criterion

The determinant criterion optimizes the coding gain. Recall that *r* is the rank of *A(c, e)*. Coding gain corresponds to the minimum r^{th} roots of the sum of the determinants of all *r*x*r* principal cofactors of *A(c, e)= B(c, e) B*(c, e)*, taken over all pairs of distinct codewords *c* and *e* [14]. Now $(\lambda_1\lambda_2 \dots \lambda_r)$ is the absolute value of the sum of determinants of all principal *r*x*r* cofactors of *A*. Thus if a diversity advantage of $r.\, n_R$ is achieved, the coding gain is$(\lambda_1\lambda_2 \dots \lambda_r)^{1/r}$. So if maximum diversity of is $n_R n_T$ the design target then we have to maximize the minimum determinant of *A(c, e)*. From the example, for the rank criterion the eigenvalues of the matrix *A* are

$\lambda_1 = -2.2679\text{-}3j$

$\lambda_2 = -5.7321\text{-}3j$

For *r*= 2, the coding gain for the codeword given in the example is 4.9327 [28].

4.3.1.3 Euclidean Distance Criterion

When the diversity gain is large (with two or more receive antennas), [29] proposes another design criteria, namely the Euclidean Distance Criteria (EDC). According to [29], the Rank and Determinant Criteria (RDC) applies to the systems with a single receive antenna and a small number of transmit antennas. This shows that with diversity gain $r.\, n_R \geq 4$, [17] shows that the error probability is upper bounded by

$$P_e(c \longrightarrow e) \leq \frac{1}{4}\exp\left(-\frac{n_R E_s}{4N_0}\sum_{i=1}^{n_T}\sum_{j=1}^{l}\left|e_j^i - c_j^i\right|\right) \qquad ; r.\, n_R \geq 4 \tag{4.15}$$

which indicates that we should maximize the minimum squared Euclidean distance between any two different codewords [29].

4.3.2 Design Criteria for STTC over Rician Fading

Equation (4.12) gives the probability of error for independent Rician distributions. If we consider (4.12) for sufficiently high signal-to-noise ratios, we get [14]

$$P(c \to e) \leq \left(\prod_{i=1}^{r} \lambda_i\right)^{-n_R} \left(\frac{E_s}{4N_0}\right)^{-rn_R} \left[\prod_{j=1}^{n_R} \prod_{i=1}^{r} \exp\left(-K_{i,j}\right)\right] \tag{4.16}$$

Thus we get a diversity of $r.n_R$ and a coding gain of

$$(\lambda_1 \lambda_2 \ldots \lambda_r)^{1/r} \left(\prod_{j=1}^{n_R} \prod_{i=1}^{r} \exp\left(-K_{i,j}\right)\right)^{1/rn_R}$$

4.3.2.1 Rank Criterion

The rank criterion for Rician channel is the same as for the Rayleigh channel [14]. We assume $\Lambda(c, e)$ denotes the sum of all determinants of the *r*x*r* principal cofactors of the matrix *A(c, e)*. Here *r* is the rank of *A(c, e)*. To achieve the maximum coding gain the minimum of the products

$$\Lambda(c, e)^{1/r} \left(\prod_{j=1}^{n_R} \prod_{i=1}^{r} \exp\left(-K_{i,j}\right)\right)^{1/rn_R}$$

taken over all pairs of codewords *c* and *e* has to be maximized.

4.3.3 Design Criteria for STTC over Nakagami Fading Channels

In the multipath fading channel model literature, the Rayleigh and Rician distributions are frequently used. However, the Nakagami model is often more versatile than the above-mentioned channels [20]. In this model it is assumed that the received signal is the sum of vectors with random amplitudes and random phases. This assumption makes this model more flexible than the Rayleigh and Rician distributions [30]. The Nakagami distribution [20] is given by

$$P(\alpha) = \frac{2}{\Gamma(\mathrm{m})} \left(\frac{m}{\Omega}\right)^{m} \alpha^{2m-1} e^{-\alpha^2 m/\Omega} \tag{4.17}$$

where Γ(*x)* denotes the Gamma function of x, and

$$\Omega = E[\alpha^2]$$

The notation *E*[*x*] denotes the expected value of *x.* The constant *m* is called the inverse fading parameter, with *m* =1 corresponding to Rayleigh fading and and *m* = ∞ corresponding to no fading and defined as,

$$m = \frac{\Omega^2}{E[(\alpha^2 - \Omega)^2]} \quad ; \; m \geq \frac{1}{2} \tag{4.18}$$

The relationship between the Rician fading factor '*K*' and the Nakagami-*m* fading factor '*m*' is

$$K = \frac{\sqrt{m^2 - m}}{m - \sqrt{m^2 - m}} \; \Rightarrow \; m = \frac{K^2 + 2K + 1}{2K + 1} \tag{4.19}$$

4.3.3.1 Independent Fading

The amplitudes of $h_{i,j}$ are identical and independent *m*-distributed with the same m and Ω. PEP is given by [20],

$$P(c \longrightarrow e) \leq \frac{\left(\frac{m}{\Omega}\right)^m}{\Gamma(m)} \left(\prod_{j=1}^{m} \prod_{i=1}^{n} \frac{\Gamma(m)}{\left(\frac{E_s}{4N_0}\lambda_i + \frac{m}{\Omega}\right)^m} \right) \tag{4.20}$$

Here $\Gamma(m)$ is gamma function which means $\Gamma(n) = \int_0^\infty t^{n-1} e^{-t} dt$, $n > 0$.

$$P(c \longrightarrow e) \leq f(m) \left(\prod_{i=1}^{r} \left(\lambda_i + \frac{4N_0 m}{E_s \Omega} \right) \right)^{-m\, n_R} \left(\frac{E_s}{4N_0} \right)^{-r\, m\, n_R}$$

$$\leq f(m) \left(\prod_{i=1}^{r} \lambda_i \right)^{-m\, n_R} \left(\frac{E_s}{4N_0} \right)^{-r\, m\, n_R} \tag{4.21}$$

Here $f(m)$ is defined as [20]

$$f(m) = \left(\frac{m}{\Omega}\right)^{m - m\, n_R (n_T - r)} \Gamma(m)^{n_T n_R - 1} \tag{4.22}$$

From (4.21), the diversity order is rmn_R. This is in fact m times the diversity order that can be achieved in Rayleigh fading. The coding gain [20] is

$$f(m) = \left(\frac{m}{\Omega}\right)^{-1/r\, m\, n_R} \left(\prod_{i=1}^{r} \lambda_i\right)^{1/r} \tag{4.23}$$

Now for m =1, $\Omega = 1$ we simplify (4.21) and (4.23) as [20]

$$P(c \longrightarrow e) \leq \left(\prod_{i=1}^{r} (\lambda_i)\right)^{-n_R} \left(\frac{E_s}{4N_0}\right)^{-r\, n_R} \tag{4.24}$$

This agrees with (4.16) which is the error probability for Rayleigh fading. If we compare (4.21) and (4.23) we see that the only difference between them is the factor *f(m)* and *m* on the right hand side of (4.21). Thus we can say that the diversity order achieved in Rayleigh fading increases by a factor of *m* in Nakagami fading and the coding gain is multiplied by a factor of $(m)^{-1/rmn_R}$. We can consider this factor as the additional coding gain due to Nakagami fading [20].

4.3.3.2 Correlated Fading

In this section we present the design criteria for STTC in correlated fading. We considered the case when the fading coefficients, $h_{i,j}$ are correlated. We assume that the envelopes of $h_{i,j}$ are modeled as identically correlated Nakagami distributed random variables [20]. In [20] it is shown that rank and determinant criteria is similar to the independent Nakagami fading criteria.

4.4 Code Search with the Performance Criteria

The RDC and EDC are usually used to guide the computer search for good space-time trellis codes. Many search results are given in [16], [17], [29], [37] and [38]. Some of these are simulated in this thesis. Because of the computational complexity of the pair-wise error probability bound equations, computer simulation is usually carried out to more accurately evaluate the code performance. Performance criteria in the presence of channel estimation errors and multipath effects are discussed in [39]. It was shown that the design criteria also apply to Nakagami fading channels in [20]. The performance

criteria and simulation results for STTC over frequency selective fading channels was presented in [20].

In the following tables we present the codes designed by Tarokh et al. in [14], [24] and the codes designed by Chen et al. in [17] and [29]. These tables also give the number of states (2^v), the minimum rank *(r)* the minimum determinant (det) and the minimum squared Euclidean distance (d_{min}^2). Tables 1 and 3 presents the 4,8,16 and 32-state 4-PSK and 8-PSK STTC codes proposed by Tarokh et al. [14] [24] for a system with two transmit antennas. These codes were designed using the rank and determinant criteria (RDC). From the tables we can see these codes have full rank $r = n_T$ and maximum minimum determinant of the code distance matrices $A(c, e)$. Tables 2 and 4 present the 4,8,16 and 32-state 4-PSK and 8-PSK STTC codes proposed by Chen et al. [17] [29] for a system with two transmit antennas. These codes were designed using the Euclidean distance criteria (EDC). The code design using RDC for wireless systems with transmit antennas $n_T \geq 3$ is quite complex [29], so for this case the EDC was used in [29] to design codes. Tables 5 and 6 present the 4,8,16 and 32-state 4-PSK STTC codes proposed by Chen et al. [29] for systems with 3 and 4 transmit antennas, respectively. From these tables it is evident that the codes based on the EDC have the same value for *r*, but they have a larger Euclidean distance (d_{min}^2) compared with the codes designed based on RDC.

TABLE 1

4-PSK Trellis codes for two transmit antennas proposed by Tarokh et al. [14]

2^v	a_0^1, a_0^2	a_1^1, a_1^2	a_2^1, a_2^2	a_3^1, a_3^2	b_0^1, b_0^2	b_1^1, b_1^2	b_2^1, b_2^2	b_3^1, b_3^2	R	det	d_{min}^2
4	(0,2)	(2,0)	--	--	(0,1)	(1,0)	--	--	2	4	4
8	(0,2)	(2,0)	--	--	(0,1)	(1,0)	(2,2)	--	2	12	8
16	(0,2)	(2,0)	(0,2)	--	(0,1)	(1,2)	(2,0)	--	2	12	8
32	(0,2)	(2,0)	(3,3)	--	(0,1)	(1,1)	(2,0)	(2,2)	2	12	12

TABLE 2

4-PSK Trellis codes for two transmit antennas proposed by Chen et al. [17]

2^v	a_0^1, a_0^2	a_1^1, a_1^2	a_2^1, a_2^2	a_3^1, a_3^2	b_0^1, b_0^2	b_1^1, b_1^2	b_2^1, b_2^2	b_3^1, b_3^2	R	det	d_{min}^2
4	(0,2)	(1,2)	--	--	(2,3)	(2,0)	--	--	2	4	10
8	(2,2)	(2,1)	--	--	(2,0)	(1,2)	(0,2)	--	2	8	12
16	(1,2)	(1,3)	(3,2)	--	(2,0)	(2,2)	(2,0)	--	2	8	16
32	(0,2)	(2,3)	(1,2)	(3,2)	(2,2)	(1,2)	(2,3)	(2,0)	2	20	16

TABLE 3

8-PSK Trellis codes for two transmit antennas proposed by Tarokh et al. [14]

2^v	a_0^1, a_0^2	a_1^1, a_1^2	b_0^1, b_0^2	b_1^1, b_1^2	b_2^1, b_2^2	c_0^1, c_0^2	c_1^1, c_1^2	c_2^1, c_2^2	r	det	d_{min}^2
8	(0,4)	(4,0)	(0,2)	(2,0)	--	(0,1)	(5,0)	--	2	2	4
16	(0,4)	(4,4)	(0,2)	(2,2)	--	(0,1)	(5,1)	(1,5)	2	3.515	6
32	(0,4)	(4,4)	(0,2)	(2,2)	(2,2)	(0,1)	(5,1)	(3,7)	2	3.515	8

TABLE 4

8-PSK Trellis codes for two transmit antennas proposed by Chen et al. [17]

2^v	a_0^1, a_0^2	a_1^1, a_1^2	b_0^1, b_0^2	b_1^1, b_1^2	b_2^1, b_2^2	c_0^1, c_0^2	c_1^1, c_1^2	c_2^1, c_2^2	r	det	d_{min}^2
8	(2,1)	(3,4)	(4,6)	(2,0)	--	(0,4)	(4,0)	--	2	2	7.172
16	(2,4)	(3,7)	(4,0)	(6,6)	--	(7,2)	(0,7)	(4,4)	2	0.686	8
32	(0,4)	(4,4)	(0,2)	(2,3)	(2,2)	(3,0)	(2,2)	(3,7)	2	2.343	8.586

TABLE 5

4-PSK Trellis codes for three transmit antennas proposed by Chen et al. [29]

2^v	a_0^1, a_0^2, a_0^3	a_1^1, a_1^2, a_1^3	b_0^1, b_0^2, b_0^3	b_1^1, b_1^2, b_1^3	c_0^1, c_0^2, c_0^3	c_1^1, c_1^2, c_1^3	c_2^1, c_2^2, c_2^3	r	det	d_{min}^2
4	(0,2,2)	--	(2,3,3)	--	(1,2,3)	(2,0,2)	--	2	0	16
8	(2,2,2)	--	(2,0,3)	(1,2,0)	(2,1,1)	(0,2,2)	--	2	0	20
16	(1,2,1)	(2,2,0)	(2,0,2)	(3,2,1)	(1,3,2)	(2,0,2)	--	2	0	24
32	(0,2,2)	(1,2,2)	(2,2,0)	(1,2,2)	(2,3,3)	(2,3,1)	(2,0,0)	2	0	24

TABLE 6

4-PSK Trellis codes for four transmit antennas proposed by Chen et al. [29]

2^v	$a_0^1, a_0^2,$ a_0^3, a_0^4	$a_1^1, a_1^2,$ a_1^3, a_1^4	$b_0^1, b_0^2,$ b_0^3, b_0^4	$b_1^1, b_1^2,$ b_1^3, b_1^4	$c_0^1, c_0^2,$ c_0^3, c_0^4	$c_1^1, c_1^2,$ c_1^3, c_1^4	$c_2^1, c_2^2,$ c_2^3, c_2^4	R	det	d_{min}^2
4	(0,2,2,0)	--	(2,3,3,2)	--	(1,2,3,2)	(2,0,2,1)	--	2	0	20
8	(2,2,2,2)	--	(2,0,3,1)	(1,2,0,3)	(2,1,1,2)	(0,2,2,1)	--	2	0	26
16	(1,2,1,1)	(2,2,0,0)	(2,0,2,2)	(3,2,1,2)	(1,3,2,2)	(2,0,2,2)	--	3	0	32
32	(0,2,2,2)	(1,2,2,0)	(2,2,0,1)	(1,2,2,1)	(2,3,3,2)	(2,3,1,0)	(2,0,0,2)	3	0	36

4.5 STTC Decoder

The decoder is based on the Viterbi algorithm, so it uses the trellis structure of the code. Each time the decoder receives a pair of channel symbols it computes a metric to measure the "distance" between what is received and all of the possible channel symbol pairs that could have been transmitted. For hard decision Viterbi decoding the Hamming distance is used, and the Euclidean distance is used for soft decision Viterbi decoding. The metric values computed for the paths between the states at the previous time instant and the states at the current time instant are called "branch metrics". We assume that the decoder has ideal channel state information (CSI) and thus knows the path gains $h_{i,j}$ .If the signal is r_t^j at receive antenna j and time t , the branch metric for a transition labeled $x_t^1 x_t^2 \ldots x_t^{n_T}$ is given by [14]

$$\sum_{j=1}^{n_R} \left| r_t^j - \sum_{i=1}^{n_T} h_{i,j} q_t^i \right|^2 \; n_T \tag{4.25}$$

The Viterbi algorithm determines the path with the lowest accumulated metric.

4.6 Performance Evaluation

In MATLAB simulation we considered the IS-136 standard. The source transmitted symbols were carried out through frames length of 130 i.e. each frame consists of 130 symbols. The decoding depth of Viterbi algorithm with 20 state transitions was used to decode received signals. We also assumed ideal channel state information (CSI) is available at the receiver. It impossible to run the simulation for an infinite length of time, so we take total number of transmitted frame as a very large number. The maximum number of iterations used was 11,000 for a FER and BER above 10^{-3}. The FER is given by

$$P_e = \lim_{F \to \infty} \frac{F_e}{F} \tag{4.26}$$

Where F is the total number of transmitted frames and F_e is the total number of erroneous frames received at the receiver. Similarly BER is given by

$$P_b = \lim_{B \to \infty} \frac{B_e}{B} \tag{4.27}$$

Where B is the total number of transmitted bits and B_e is the total number of erroneous bits received at the receiver. Also SER is given by

$$P_s = \lim_{S \to \infty} \frac{S_e}{S} \tag{4.28}$$

Where S is the total number of transmitted symbols and S_e is the total number of erroneous symbols received at the receiver.

Using QPSK modulation technique for codes of table 1 and table 3 the simulation results is shown in figure 4.8 with two transmit and one receive antenna. For FER of 10^{-1}, 8-state of trellis is 1.34 dB better than 4-state trellis, 32-state trellis is 1.57 dB better than 8-state of trellis and 64-state trellis is 1.94 dB better than corresponding 32-state trellis. From simulation results it is clear that performance of the system improves with increase in number of states of trellis i.e. it shows low frame error rate as level of states for trellis were increased.

In this thesis different design criteria for STCs were reviewed. As discussed, the design criteria for quasi-static Rayleigh fading channels depends on the rank of the codeword distance matrix r, and the number of receive antennas in the system, n_R. It was also briefly discussed that if $rn_R < 4$, then the *rank & determinant* criterion is suitable, else it's more appropriate to use the *trace* criterion.

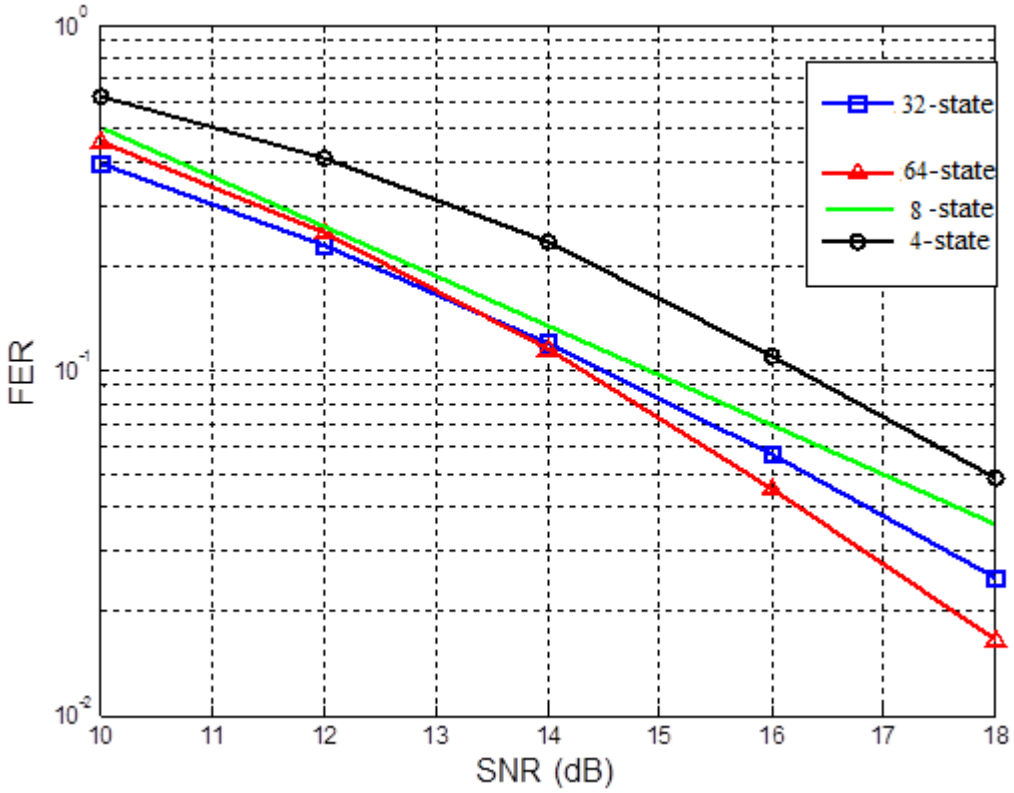

Figure 4.8. Performance of STTC with 2-tx and 1-rx antenna using QPSK modulation schemes.

For simulation purpose we have generated the Nakagami fading by using sum of sinusoidal using Rayleigh and Rician fading as given in [14] Equation 6. The received signal for Nakagami can be expressed as :

$$R_{nakagami} = R_{ray}\mathrm{e}^{1-m} + R_{rice}(1 - \mathrm{e}^{1-m}) \tag{4.29}$$

Where R_{ray} and R_{rice} are envelops of Rayleigh and Rician channels respectively. By adopting sum of sinusoidal approach for received signal generation and expressing it in inphase and quadrature form for both Rayleigh and Rician fading.

$$R(t) = \sqrt{[I(t)]^2 + [Q(t)]^2} \tag{4.30}$$

Where *I(t)* and *Q(t)* are the inphase and quadrature components [44].

As shown in Figure 4.9 performance of Nakagami channel is better increased as we increase number of transmits antennas for fixed number of receivers. Here if we transmit information over 4 transmit antenna gives better performance than transmitted through 2

and 3 antenna. So increasing number of transmit antenna at base station is better option than increasing receiving antennas for high throughput.

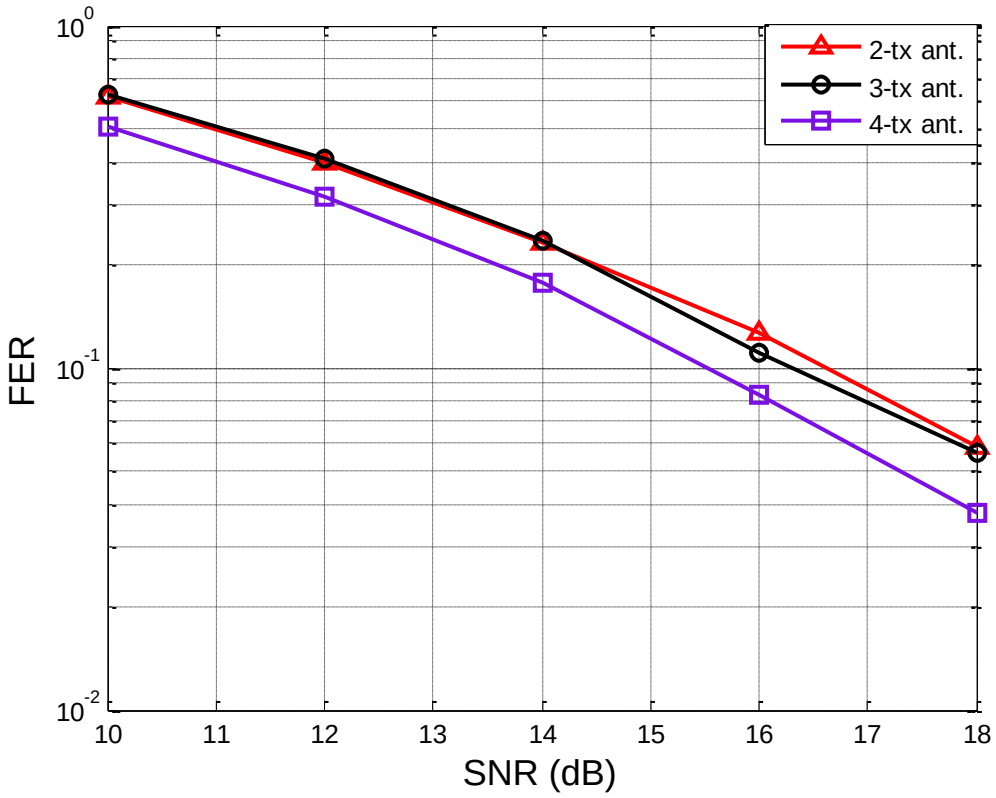

Figure 4.9. Performance of 4-state QPSK STTCs over Nakagami fading channel for m=2, and different transmit antennas (2-tx, 3-tx, 4-tx) and one receive antenna.

Figure 4.10 shows that for a system with $n_T = 2$ and $n_R = 2$, the 4-state code for m = 1, 2 and 8. In special case for m=1 the performance of Nakagami is equivalent to Rayleigh performance. It is shown in figure 4.10, when value of m is increased the performance of the STTCs increases accordingly. There is not much significant effect on performance of STTCs can be found for m > 6, that's why value of m is consider between 0.5 to 10. For m >10, Nakagami fading does not affect the code performance.

As mentioned earlier, if $rn_R < 3$, the Euclidean distance does not dominate the performance [29]. In the code design for 4-PSK signal sets, generator coefficients are determined through exhaustive search. Since the encoder structure cannot guarantee geometrical uniformity of the code, the search was based on all possible pairwise error events. In order to reduce the complexity of the code search, we use the determinants of the known codes in [38] as the bench marks. The complexity of the code construction is

the same as that for previously known codes [38]. All these codes have full rank of r = 2. The codes are described by memory order (v), generator coefficients g_1, g_2).

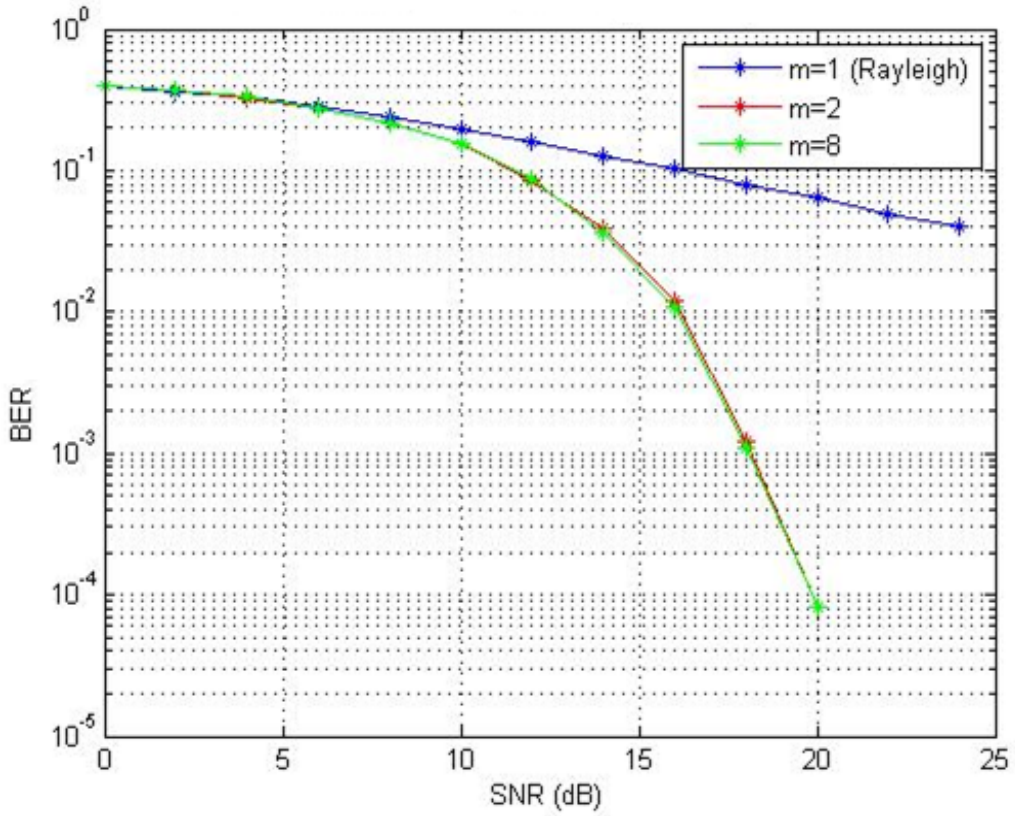

Figure 4.10. Performance of 4-state QPSK STTCs over Nakagami fading channel for 2-tx, 2-rx antennas.

Figure 4.11 shows the performance of Rayleigh, Rician and Nakagami in fast fading channels environment. For FER of 10^{-1} Rayleigh's (m=1) SNR is at 15.51 dB, Rician's (m=2 ≅ K= 2.414) SNR at 14.73 dB and Nakagami's (m=6) SNR at 12.72 dB which means Rician's performance is 0.78 dB better than Rayleigh's performance and Nakagami's performance is 2.01 dB better than Rician and 2.79 dB better than Rayleigh's performance. Thus for fast fading channel, performance of Nakagami channel outperforms the Rayleigh and Rician channel's performance.

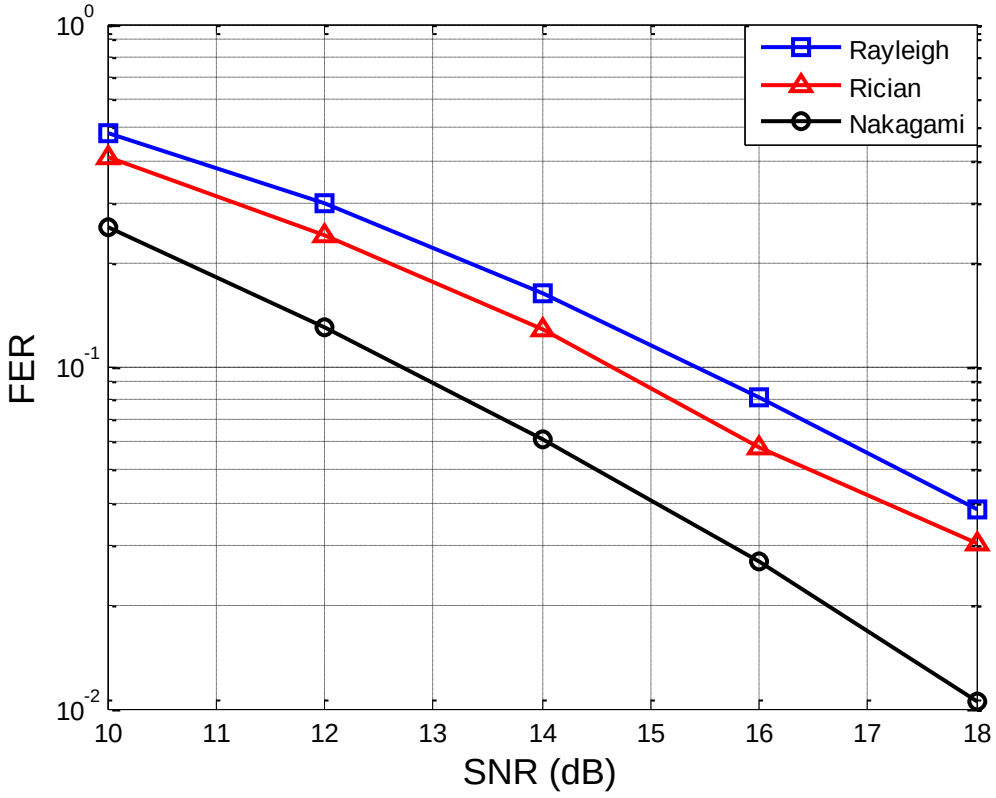

Figure 4.11. Performance of Rayleigh, Rician and Nakagami in fast fading channels for 4-state, 2-tx, 2-rx STTC using QPSK.

Figure 4.12 shows the performance for 4-state, QPSK STTCs in slow fading environment at FER of 10^{-3}. At FER of 10^{-1} Rician performance is 3.14 dB SNR better than Nakagami's performance. Also Rayleigh performance is 9.62 dB SNR better than Rician's performance. Nakagami channel perform worse in slow fading since it is 12.76 dB SNR worse than corresponding Rayleigh channel's performance. Thus as shown in figure 4.12, for slow fading channel performance of Rayleigh channel outperforms the Rician and Nakagami channel's performance. Also it can be seen that Nakagami channel fading response is worse than the other counterpart's performance too.

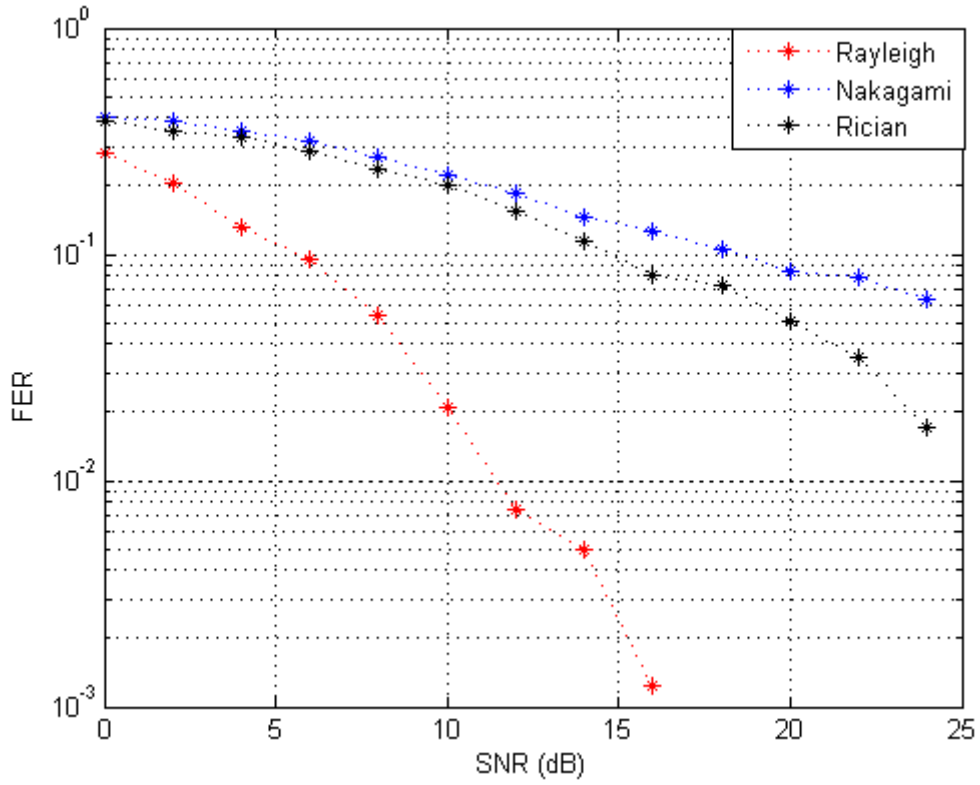

Figure 4.12. Performance of 4-state QPSK STTCs of Rayleigh, Rician and Nakagami in slow fading channels for 2-tx and 2-rx antennas.

4.7 Summary of Space Time Trellis Codes

We show how the problem of finding union bounds is reduced to problem of finding moment generating function (characteristic function) of SNR under various channel conditions. Section 4.1 of this chapter gave a brief description of a STTC based wireless system. We showed and explained the transmitter and receiver of such system. Section 4.2 gave an explanation of the construction of a STTC. In the beginning of this section we gave a simple example of how information is coded in STTC based systems. Later we discussed code construction and the encoder structure of 4-state 4-PSK and 8-state 8-PSK STTC. In Section 4.3 we discussed about different performance criterion. We presented a details of the RDC and EDC, and provided design criteria over Rayleigh, Rician and Nakagami fading. In Section 4.4 we presented the codes designed by Tarokh et al. and Chen et al. in six tables. Section 4.5 briefly discussed STTC decoders. Section 4.6 describes about performance evaluation mathematically in MATLAB according to IS-136 standard. Several simulations were discussed which were carried out according to mathematical and numerical data.

The design criteria for code construction of STTC assume that perfect CSI is available at the receiver, i.e., the receiver knows the exact channel path gains. In reality, it is impossible for the receiver to have perfect channel information; however the receiver can estimate CSI. Due to estimation errors performance degradation will occur. Several techniques have been introduced to estimate the channel [31], [32] and [33]-[36].

Earlier in our discussion we mentioned that the Nakagami fading channel is more flexible than Rayleigh and Rician channels. For this reason we presented more simulation results on the performance of STTCs over Nakagami channels. It was determined that the design criteria for space-time trellis codes over Rayleigh fading channels is suitable for both independent and correlated Nakagami fading channels.

CHAPTER 5

CONCLUSION AND FUTURE SCOPE

In this final chapter, we provide the summary of the work described in previous chapters followed by the conclusion of this thesis.

5.1 Summary and Conclusion

Space time trellis codes perform better than all other counterparts because of no bandwidth expansion and high spectral efficiency. The need to achieve reliable wireless systems with high spectral efficiency, low complexity and good error performance results in continued research in this field. Recently, MIMO wireless systems can achieve impressive increases in overall system performance. The potential to provide the next major leap forward for wireless communications has led this technology to becoming the next frontier of wireless communications. As a result, it has received the attention not only of the international R&D community, but also of the wireless communications industry. This is evidenced from the international standardization efforts in the context of UMTS (e.g., 3GPP) and IEEE 802.11 (for wireless LANs) and also in the context of proposals for next generation (4G and beyond) wireless systems. The chapters are organized so the reader builds upon the information provided and gradually reaches a point where more complex (system) issues are discussed. If readers wish to study further specific aspects of MIMO technology will find the references cited in each chapter particularly useful.

This thesis introduces the principles of MIMO systems employing the necessary mathematical analysis to consider the achieved capacity performance. In this context, flat fading across time and frequency is considered, and the Rayleigh model is employed for describing the wireless channel. Furthermore, the case of spatial selective fading is examined by considering LOS propagation, with the Rician model and combines both Rician and Rayleigh model to form Nakagami model. The mathematical representation of the MIMO system is performed through a complex matrix, which depends on the scenario considered each time (i.e., flat or selective spatial fading). The capacity achieved by the MIMO channel in all the above cases is studied with the use of the Shannon extended capacity formula. The capacity performance results, developed from the simulations

performed, are related to the number of the multiple antenna elements that the Rx and the Tx are equipped with, the distance between them and the degree of correlation evidenced.

In this work it is shown that if number of states of trellis is increased there will be corresponding performance of system increased. It has been shown if number of transmit antenna were increased from 2,3 up to 4 at base station for fixed single receiver in Nakagami fading channel environment then there is improvement in the throughput of the systems performance. This reduces the burden of increasing the receiving antennas. If m-factor of Nakagami fading increases up to certain level it improves the performance of the system and if m=1 or Rician fading factor K=0 for special case it corresponds to equivalent Rayleigh fading. For fast fading, 2-tx, 2-rx 4-state QPSK Nakagami fading channel's performance is 2.01 dB better than Rician and 2.79 dB of SNR better than Rayleigh fading channel's performance. Also for slow fading, 2-tx, 2-rx 4-state QPSK Nakagami fading channel's performance is 12.76 dB and 9.62 dB worse than corresponding Rayleigh and Rician fading channel's performance. It is concluded that Nakagami fading channel gives better performance over Rayleigh and Rician fading channels in fast fading environment and Rayleigh outperforms performance over Rician and Nakagami in slowly fading environment.

5.2 Future Scope

STTC codes are computationally very demanding because of its high throughput. Therefore, a procedure needs to be developed to ease decoding if STTC codes need to be used for practical purposes. Therefore, the idea of this dissertation work will be to bridge this gap of high decoding complexity by disintegrating the coding structure.

Possible future work and research can be carried out for the cases of multiple receive antennas, higher order modulation, different types of fading, and imperfect channel estimation. The Matlab script that was used for Viterbi decoding could be optimized so that simulation times could be significantly reduced.

REFERENCES

[1] G.J. Foschini and M.J. Gans, "On limits of wireless communications in a fading environment when using multiple antennas," *Wireless Personal Communications*, vol. 6, 1998, pp. 311–335.

[2] E. Telatar, "Capacity of multi-antenna Gaussian channels," *European Transactions on Telecommunications*, vol. 10, no. 6, Nov./Dec. 1999, pp. 585–595.

[3] G.J. Foschini, "Layered space-time architecture for wireless communications in a fading environment when using multiple antennas," *Bell Labs. Tech. J.*, vol. 6, no. 2, pp. 41–59, 1996.

[4] C.E. Shannon, "A mathematical theory of communication," *Bell Syst. Tech. J.*, vol. 27, pp. 379–423 (Part one), pp. 623–656 (Part two), Oct. 1948, reprinted in book form, University of Illinois Press, Urbana, 1949.

[5] C. Berrou, A. Glavieux and P. Thitimajshima, "Near Shannon limit error-correcting coding and decoding: turbo codes," in *Proc. 1993 Inter. Conf Commun.*, 1993, pp. 1064–1070.

[6] R.G. Gallager, "Low Density Parity Check Codes," MIT Press, Cambridge, Massachusets, 1963.

[7] D.C. MacKay, "Near Shannon limit performance of low density parity check codes," *Electronics Letters*, vol. 32, pp. 1645–1646, Aug. 1966.

[8] "Framework and overall objectives of the future development of IMT-2000 and systems beyond IMT-2000," *ITU-R Recommendation M.1645*, June. 2003.

[9] I. Lee, C.-E. W. Sundberg, M. Sawahashi, S. Glisic, and S. McLaughlin, \Guest editorial: "4G wireless system," *IEEE J. Select. Areas Commun.*, vol. 24, no. 3, pp. 413{418, Mar. 2006.

[10] Craig, J. W. "A new, simple and exact result for calculating the probability of error for two-dimensional signal constellations," *IEEE MILCOM*, 1991, 25.5.1–25.5.5.

[11] B. Vucetic, and J. Yuan, Space-time coding, John Wiley & Sons Ltd, 2003.

[12] Sklar, B. (2002) Digital Communications: Fundamentals and Applications 2/E, Prentice Hall.

[13] Rappaport, T.S. (2001) Wireless Communications: Principles and Practice 2/E, Prentice Hall.

[14] V. Tarokh, N. Seshadri, and A. R. Calderbank, "Space-time codes for high data rate wireless communication: Performance criterion and code construction," *IEEE Transaction on Information Theory*, vol. 44, pp. 744-765, March 1998.

[15] S.M. Alamouti, "A simple transmitter diversity scheme for wireless communications," *IEEE Journal on Selected Areas in Communications*, vol. 16, pp. 1451-1458, October 1998.

[16] S. Baro, G. Bauch, and A. Hansmann, "Improved codes for space-time trellis-coded modulation," *IEEE Communications Letters*, vol. 4, pp. 20-22, January 2000.

[17] Z. Chen, J. Yuan, and B. Vucetic, "Improved space-time trellis coded modulation scheme on slow Rayleigh fading channels," *Electronics Letters*, vol. 37, no. 7, pp. 440-441, March 2001.

[18] M. Baghaie A., P. A. Martin, and D. P. Taylor, "Grouped multilevel space-time trellis codes," *IEEE Communications Letters*, vol. 14, pp. 232-234, March 2010.

[19] Sajjad Beygi, Mohd.Mehdi Kafashan, Hamid Reza Bahrami, Tho Le Ngoc, and Mehdi Malaki, "Space Time Trellis Codes for Two way Relay MIMO Channels With Single-Antenna Relay Nodes," *IEEE transactions applying for publishing , 2013.* (Sought for permission to IEEE email: pubs-permissions@ieee.org, allows only for personal uses).

[20] Y. Gong and K. B. Letaief, "Performance of space-time trellis coding over Nakagami fading channels," *IEEE Vehicular Technology Conference,* pp. 1405-1409, Spring 2001.

[21] Jing Yang, Pingzhi Fan, Trung Q. Duong, and Xianfu Lei, "Exact Performance of Two-Way AF Relaying in Nakagami-m Fading Environment," *IEEE transactions on wireless communications,* vol. 10, no. 3, March 2011.

[22] Foschini, G. J. and Gans, M. “On the limits of wireless communication in a fading environment when using multiple antennas,” *Wireless Personal Communications*, Mar. 1998, 311–35.

[23] Wittneben, A., “A new bandwidth efficient transmit antenna modulation diversity scheme for linear digital modulation,” *IEEE International Conference on Communications (ICC)*, May 1993, 1630–4.

[24] Seshadri N, Tarokh V, Calderbank AR., “Space-time codes for wireless communication: code construction,” *IEEE 47th Vehic. Tech. Conf. Tech.*, pp. 637-641, 1997.

[25] Sklar B., Digital Communications Fundamentals and Applications, Second Edition, Upper Saddle River, NJ, Prentice Hall P T R, 2001.

[26] D. Varshney, C. Arumugam, V. Vijayaraghavan, N. Vijay and S. Srikanth, “Space-time codes in wireless communications,” vol. 22, pp.36 – 38, August-September 2003.

[27] Haykin S., Communication Systems. Delhi, India, John Wiley and Sons, 4th edition, 2001

[28] Yuen N., “Performance Analysis of Space-time Trellis codes,” Master of Engineering report, University of British Columbia, April 2000.

[29] Z. Chen, B. Vucetic, J. Yuan and Lo. Ka. Leong, “Space-time trellis codes for 4-PSK with three and four transmit antennas in quasi-static flat fading channels,” *Communication Letters*., vol. 6, no. 2, pp. 67-69, Feb. 2002.

[30] M. Nakagami, “The m-distribution: A general formula of intensity distribution of rapid fading,” in *Statistical Methods in Radio Wave Propagation*, W. G. Hoffman, Ed. Oxford, England: Pergamon, 1960.

[31] J. Zhang and P.M. Djuric, “Joint channel estimation and decoding of space-time trellis codes,” *IEEE Signal Processing Workshop on Statistical Signal Processing*, pp. 559-562, 2001.

[32] Y. Xue and X. Zhu, "Per-survivor-processing based adaptive decoder for space-time trellis code," *Acta Electronica Sinica*, vol. 29, no. 10, pp. 1352-1355, Publisher: Chinese Inst. Electron, China, Oct. 2001.

[33] Y. Xue and Z. Xuelong, "A new soft-decision adaptive decoder for space-time trellis code," *IEEE Intern. Conf. Personal Wireless Commun. Conf. Proc.*, pp. 162-166, 2000.

[34] Y. Xue and Z. Xuelong, "PSP-based decoding for space-time trellis code," *IEEE Asia-Pacific Conf. on Circuits and Systems.Electronic Commun. Systems*, pp. 783-786, 2000.

[35] M. J. Heikkila, E. Majonen and J. Lilleberg, "Decoding and performance of space-time trellis codes in fading channels with intersymbol interference," *IEEE International Symposium on Personal Indoor and Mobile Radio Communications.*, vol. 1, pp. 490-494, 2000.

[36] Y. Xue and Z. Xuelong, "PSP decoder for space-time trellis code based on accelerated self-tuning LMS algorithm," *Electronics Lett.*, vol. 36, no. 17, pp. 1472-1474, 17 Aug. 2000.

[37] D. M. Ionescu, K. K. Mukkavilli, Y. Zhiyuan and J. Lilleberg, "Improved 8- and 16-state space-time codes for 4PSK with two transmit antennas," *Commun. Lett.*, vol. 5, no. 7, pp. 301-303, July 2001.

[38] J. Yuan, Z. Chen and B. Vucetic, "Performance of space-time coding on fading channels," *IEEE Trans. Commun* , vol. 51, no. 12, pp. 1991-1996, Dec. 2003.

[39] Tarokh V, Naguib A, Seshadri N, Calderbank AR., "Space-time codes for high data rate wireless communication: performance criteria in the presence of channel estimation errors, mobility, and multiple paths," *IEEE Trans. Commun.*, vol. 47, pp. 199-207, Feb. 1999.

[40] Horn, A. H. and Johnson, C. R., Matrix Analysis, Cambridge University Press, 1999.

[41] Guey, J.-C., Fitz, M. P., Bell, M. R. and Kuo, W.-Y., "Signal design for transmitter diversity wireless communication systems over Rayleigh fading channels," *IEEE Trans. on Communications*, 47(4): Apr. 1999, 527–37.

[42] Ionescu, D. M., "New results on space-time code design criteria," *IEEE Wireless Communications and Networking Conference (WCNC)*, 1999, 684–7.

[43] Jakes, W. C. Microwave Mobile Communication, Wiley, 1974.

[44] Li Tang, Zhu Hongbo, "Analysis and Simulation of Nakagami fading channel with Matlab," *Asia-Pacific conference on environmental electromagnetic* CEEM'2003, China,pp. 490-494.

[45] M.O. Farooq, W. Li and T.A. Gulliver, "A new cellular structure with Space-Time Trellis Code," *Workshop on Wireless Circuits and Systems* (WoWCAS), Vancouver, Canada, pp. 10-11, May 21-22, 2004.

Appendix A. Generator Matrix to Trellis Converter

```
function [trellis] = gm2trellis(GM, M)
% GM2TRELLIS Convert generator matrix to trellis description
%            for encoding and decoding space-time trellis codes
%
% The GM format:
%   e.g. GM = transpose[a0 b0 c0 a1 b1 c1 c2; a0' b0' c0' a1' b1' c1' c2']
%   a0 is the most significant bit (MSB)
% Reference:
%   Z. Chen, J. Yuan, etc. "An improved space-time trellis coded modulation
%   scheme on slow rayleigh fading channels"
%
% Input paraeters:
%   GM - generator matrix
%   M - M-PSK constellation
%
% Return:
%   trellis - trellis description of the space-time trellis codes
%
% check inputs and get parameters
k = log2(M); % input/output bits per symbol
if (nargin ~= 2)
    error('Usage: [trellis] = GM2TRELLIS(GM, M)');
end
if (ndims(GM) ~= 2)
    error('Input generator matrix must be 2D matrix');
end
if (M <= 1 | k >= size(GM, 1) )
    error('Invalid M value');
end
if (k <= 0 | M < max(GM) )
    error('Invalid M value');
end
% number of states, equal to number of rows in GM minus number of input bits
s = size(GM, 1) - k;
num_states = 2^s;
% number of outputs (transmit antennas), equal to number of columns in GM
Nt = size(GM, 2);
% outputs and nextState
outputs = zeros(num_states, 2^k);
nextStates = zeros(num_states, 2^k);
% generate outputs and nextState matrix
for i=(0:num_states-1)
%state_bits = fliplr(getbits(i, s));
state_bits = (getbits(i, s));
for j=(0:2^k-1)
   % compute output
   %input_bits = fliplr(getbits(j, k));
   input_bits = (getbits(j, k));
   bits = [input_bits, state_bits];
   for t=(0:Nt-1)
   outputs(i+1, j+2^k*t+1) = mod(bits*GM(:,t+1),M);
   end
   % get next state
   next_state_bits = rightshift(state_bits, k);
   rem=mod(s,k); nshift = k-rem;
   if (rem~=0)
```

```
     for idx=(0:rem-1)
        next_state_bits(s-idx) = state_bits(s-idx-nshift);
     end
end
       next_state_bits(1:k) = input_bits;
       % save next state
       %next_state = bit2num(fliplr(next_state_bits));
       next_state = bit2num((next_state_bits));
       nextStates(i+1, j+1) = next_state;
   end
end
% the trellis structure
trellis.numInputSymbols = 2^k;
trellis.numOutputSymbols = 2^k;
trellis.numStates = num_states;
trellis.numOutputs = Nt;
trellis.outputs = outputs;
trellis.nextStates = nextStates;
% display results
%if (nargout ~= 1)
if(0)
    display(outputs)
    display(nextStates)
end
%end
% ------------------------
% helper functions
% ------------------------
function [bits] = getbits(x, n)
% get the binary bits for decimal integer inputs
% e.g. (12) => [1,1,0,0]
bits = zeros(1, n);
ind = 1;
while (x~=0)
    bits(ind) = mod(x,2);
    x = floor(x/2);
    ind = ind + 1;
end
bits = fliplr(bits);
function [y] = bit2num(x)
% convert bit streams to interger
% e.g. [1 1 0 0] => (12)
y = 0; mul = 1;
for i=(length(x):-1:1)
   y = y + mul*x(i);
   mul = mul*2;
end
function [y] = rightshift(x, k)
% shift bit streams right k times (arithmatic shift)
y = zeros(size(x));
for i=(1:length(x)-k)
   y(i+k) = x(i);
end
```

Appendix B. Space-Time Encoder Source Code

```
 Space-Time Trellis Codes (STTC) Encoder MATLAB C-Mex Function
 Calling format: [code, finalState] = stcenc(
             in, // input message symbols (column vector)
             k, // trellis: number of input bits
             n, // trellis: number of output bits
             numOutputs, // trellis: number of outputs
             numStates, // trellis: number of states
             outputs, // trellis: outputs (numStates by 2^k*numOutputs)
             nextStates, // trellis: next states (numStates by 2^k)
             initState) // trellis: initial state

#include "mex.h"
#include "math.h"
#define PI 3.14159265358979
static const char MEM_ALLOCATION_ERROR[] = "Memory allocation error.";
enum {IN_ARGC = 0, /* input message symbols */
       TRELLIS_K_ARGC, /* number of input bits */
       TRELLIS_N_ARGC, /* number of output bits */
       TRELLIS_NUM_OUTPUTS_ARGC, /* number of outputs */
       TRELLIS_NUM_STATES_ARGC, /* number of states */
       TRELLIS_OUTPUT_ARGC, /* output matrix (decimal) */
       TRELLIS_NEXT_STATE_ARGC, /* next state matrix */
       INITSTATE_ARGC, /* initial state */
       NUM_ARGS};
#define IN_ARG (prhs[IN_ARGC])
#define TRELLIS_K_ARG (prhs[TRELLIS_K_ARGC])
#define TRELLIS_N_ARG (prhs[TRELLIS_N_ARGC])
#define TRELLIS_NUM_OUTPUTS_ARG (prhs[TRELLIS_NUM_OUTPUTS_ARGC])
#define TRELLIS_NUM_STATES_ARG (prhs[TRELLIS_NUM_STATES_ARGC])
#define TRELLIS_OUTPUT_ARG (prhs[TRELLIS_OUTPUT_ARGC])
#define TRELLIS_NEXT_STATE_ARG (prhs[TRELLIS_NEXT_STATE_ARGC])
#define INITSTATE_ARG (prhs[INITSTATE_ARGC])
#define CODE_ARG (plhs[0])
#define STATE_ARG (plhs[1])
static void SttcEncode(int nlhs, mxArray *plhs[],
int nrhs, const mxArray *prhs[])
{
       /* Get input & outputs */
       int_T blockSize = (int_T)mxGetM(IN_ARG);
       int_T k = (int_T)mxGetScalar(TRELLIS_K_ARG);
       int_T n = (int_T)mxGetScalar(TRELLIS_N_ARG);
       int_T numOutputs = (int_T)mxGetScalar(TRELLIS_NUM_OUTPUTS_ARG);
       int_T numStates = (int_T)mxGetScalar(TRELLIS_NUM_STATES_ARG);
       real_T *outputs = mxGetPr(TRELLIS_OUTPUT_ARG);
       real_T *nextState = mxGetPr(TRELLIS_NEXT_STATE_ARG);
       real_T initState = (real_T)mxGetScalar(INITSTATE_ARG);
       real_T *in = mxGetPr(IN_ARG);
       real_T *rout = mxGetPr(CODE_ARG
       = mxCreateDoubleMatrix(blockSize, numOutputs, mxCOMPLEX));
       real_T *iout = mxGetPi(CODE_ARG);
       real_T *currState = mxGetPr(STATE_ARG
       = mxCreateDoubleMatrix(1,1,mxREAL));
       int_T M = 1<<n;
       int_T indx1;
       const char *msg = NULL;
       /* Verify memory allocation */
       if(rout == NULL){
```

```
            msg = MEM_ALLOCATION_ERROR;
            goto EXIT_POINT;
        }
        if(iout == NULL){
            msg = MEM_ALLOCATION_ERROR;
            goto EXIT_POINT;
        }
if(currState == NULL){
    msg = MEM_ALLOCATION_ERROR;
    goto EXIT_POINT;
}
/* setup initial state */
currState[0] = initState;
/* Loop through all input symbols */
for(indx1 = 0; indx1 < blockSize; indx1++){
   int_T indx2;
   /* Loop through all outputs */
   for(indx2 = 0; indx2 < numOutputs; indx2++){
      /* Calculate offsets */
       int_T bOffset = blockSize * indx2;
       int_T cOffset = numStates * ( (int_T)in[indx1] + indx2*(1<<k) );
       /* Get output */
       real_T code = outputs[((int_T)currState[0])+cOffset];
       /* Map to inphase and quadrature components using M-ary PSK
       constellation*/
       /* the average energy for the constellations points is sqrt(Es) = 1 */
       rout[indx1+bOffset] = cos(2.0*PI*code/M);
       iout[indx1+bOffset] = sin(2.0*PI*code/M);
  }
  /* Get next state */
       currState[0] =
nextState[(int_T)currState[0]+(((int_T)in[indx1])*numStates)];
}
EXIT_POINT:
    if(msg != NULL){
      mexErrMsgTxt(msg);
  }
}
static void CheckParameters(int nlhs, mxArray *plhs[],
int nrhs, const mxArray *prhs[])
{
       int_T k = (int_T)mxGetScalar(TRELLIS_K_ARG);
       int_T n = (int_T)mxGetScalar(TRELLIS_N_ARG);
       int_T numOutputs = (int_T)mxGetScalar(TRELLIS_NUM_OUTPUTS_ARG);
       int_T numStates = (int_T)mxGetScalar(TRELLIS_NUM_STATES_ARG);
       int_T nrow, ncol;
       const char *msg = NULL;
  /* Check number of parameters */
  if(nrhs != 8){
       msg = "Invalid number of input arguments.";
       goto EXIT_POINT;
 }
if(nlhs > 2){
    msg = "Invalid number of output arguments.";
    goto EXIT_POINT;
 }
/* Check input demension */
nrow = (int_T) mxGetN(IN_ARG);
   if(nrow != 1){
       msg = "Input message must be a column vector.";
       goto EXIT_POINT;
 }
/* Check trellis outputs */
ncol = (int_T) mxGetM(TRELLIS_OUTPUT_ARG);
nrow = (int_T) mxGetN(TRELLIS_OUTPUT_ARG);
if( ncol != numStates || nrow != numOutputs*(1<<k) ){
       msg = "Incorrect size of trellis outputs table.";
```

```
        goto EXIT_POINT;
 }
/* Check trellis nextStates */
ncol = (int_T) mxGetM(TRELLIS_NEXT_STATE_ARG);
nrow = (int_T) mxGetN(TRELLIS_NEXT_STATE_ARG);
if(ncol != numStates || nrow != 1<<k ){
        msg = "Incorrect size of trellis nextStates table.";
        goto EXIT_POINT;
 }
EXIT_POINT:
    if(msg != NULL){
        mexErrMsgTxt(msg);
 }
}/* CheckParameters */
void mexFunction(int nlhs, mxArray *plhs[],
        int nrhs, const mxArray *prhs[])
{
        CheckParameters(nlhs, plhs, nrhs, prhs);
        SttcEncode (nlhs, plhs, nrhs, prhs);
}
```

Appendix C. Space-Time Decoder Source Code For 4PSK, 4-State Case

```
function [fer, ser] = qpsk4state21(Nt, Nr, trellis, maxFrameErr)
% 2Tx 1Rx diversity scheme without channel estimation errors, 4PSK, 4state
% Filename: qpsk4state21.m
% Last edited: JUNE 19, 2014
% By Kiran Joshi
       .
       .
       .
% MLSE Decoding with the Viterbi algorithm
% Initialize the partial metric for each state to 0.
for (j=1:numStates)
    partMet(j) = 0;
end
%State (predecessor) history table. The entries for each array is a state (ie. 0
to % M-1).
stateHist = zeros(numStates,size(msg,1));
%stateHist(A,i)=B reads "The state at time i is A, and it comes from state B".
%State sequence table
stateSeq = ones(1,size(msg,1)+1); %1x(frameLength+1)
%stateSeq(frameLength+1) = 0;
% Loop through each input symbol and determine the survivor for each state
for (i=1:size(msg,1))
    if (i==1) %at the beginning
      for (state=1:numStates)
       surv(state,2*i-1)=0;
       surv(state,2*i)=state;
       tmp_surv(state,2*i-1)=0;
       tmp_surv(state,2*i)=state;
       %calculate branch metrics
       brMet(i,state) = (abs(chanOut(i) - h(1)*in(i) - h(2)*in(state))).^2;
       %update partial metrics
       partMet(state) = brMet(i,state);
       %update state history table
       stateHist(state,i) = 1;
    end
  elseif (i==frameLength) %at the end
    %calculate branch metrics
    for (state=1:numStates)
       brMet(state,1) = (abs(chanOut(i) - h(1)*in(state) - h(2)*in(1))).^2;
       %update the partial metrics
       partMet(1,state) = partMet(state) + brMet(state,1);
       %update survivors
       partMetArray(state) = [partMet(1,state)];
    end
[minVal, minIndex] = min(partMetArray);
if (minIndex == 1) %00 branch is survivor
       surv(1) = [tmp_surv(1)];
       surv(1,2*i-1)=0; surv(1,2*i)=0;
       stateHist(1,i) = 1;
elseif (minIndex == 2) %10 branch is survivor
       surv(1) = [tmp_surv(2)];
       surv(1,2*i-1)=1; surv(1,2*i)=0;
       stateHist(1,i) = 2;
elseif (minIndex == 3) %20 branch is survivor
       surv(1) = [tmp_surv(3)];
       surv(1,2*i-1)=2; surv(1,2*i)=0;
       stateHist(1,i) = 3;
else %30 branch is survivor
```

```
        surv(1) = [tmp_surv(4)];
        surv(1,2*i-1)=3; surv(1,2*i)=0;
        stateHist(1,i) = 4;
    end
else %i = [2:frameLength-1]
 %% STATE 0 %%
 %Calculate branch metrics going into state 0
 for (state=1:numStates)
    brMet(state,1) = (abs(chanOut(i) - h(1)*in(state) - h(2)*in(1))).^2;
    %Calculate partial metrics going into state 0
    tmpPartMet(1,state) = partMet(state) + brMet(state,1);
  end
  %update survivors
  [minVal(1), minIndex(1)] = min([tmpPartMet(1,1) tmpPartMet(1,2)
tmpPartMet(1,3)
  tmpPartMet(1,4)]);
   if (minIndex(1) == 1) %00 branch is survivor
        surv(1) = [tmp_surv(1)];
        surv(1,2*i-1)=0; surv(1,2*i)=0;
  elseif (minIndex(1) == 2) %10 branch is survivor
        surv(1) = [tmp_surv(2)];
        surv(1,2*i-1)=1; surv(1,2*i)=0;
  elseif (minIndex(1) == 3) %20 branch is survivor
        surv(1) = [tmp_surv(3)];
        surv(1,2*i-1)=2; surv(1,2*i)=0;
  else %30 branch is survivor
        surv(1) = [tmp_surv(4)];
        surv(1,2*i-1)=3; surv(1,2*i)=0;
  end
  %update state history table for state 0
  stateHist(1,i) = minIndex(1);
  %% STATE 1 %%
  %Calculate branch metrics going into state 1
  for (state=1:numStates)
        brMet(state,2) = (abs(chanOut(i) - h(1)*in(state) - h(2)*in(2))).^2;
        %calculate partial metrics going into state 1
        tmpPartMet(2,state) = partMet(state) + brMet(state,2);
  end
  %update survivors
  [minVal(2), minIndex(2)] = min([tmpPartMet(2,1) tmpPartMet(2,2)
tmpPartMet(2,3)
tmpPartMet(2,4)]);
  if (minIndex(2) == 1) %01 branch is survivor
        surv(2) = [tmp_surv(1)];
        surv(2,2*i-1)=0; surv(2,2*i)=1;
  elseif (minIndex(2) == 2) %11 branch is survivor
        surv(2) = [tmp_surv(2)];
        surv(2,2*i-1)=1; surv(2,2*i)=1;
  elseif (minIndex(2) == 3) %21 branch is survivor
        surv(2) = [tmp_surv(3)];
        surv(2,2*i-1)=2; surv(2,2*i)=1;
  else %31 branch is survivor
        surv(2) = [tmp_surv(4)];
        surv(2,2*i-1)=3; surv(2,2*i)=1;
  end
  %update state history table for state 1
  stateHist(2,i) = minIndex(2);
  %% STATE 2 %%
  %Calculate branch metrics going into state 2
  for (state=1:numStates)
     brMet(state,3) = (abs(chanOut(i) - h(1)*in(state) - h(2)*in(3))).^2;
     %Calculate partial metrics going into state 2
     tmpPartMet(3,state) = partMet(state) + brMet(state,3);
  end
  %update survivors
  [minVal(3), minIndex(3)] = min([tmpPartMet(3,1) tmpPartMet(3,2)
tmpPartMet(3,3)
tmpPartMet(3,4)]);
```

```
  if (minIndex(3) == 1) %02 branch is survivor
       surv(3) = [tmp_surv(1)];
       surv(3,2*i-1)=0; surv(3,2*i)=2;

  elseif (minIndex(3) == 2) %12 branch is survivor
       surv(3) = [tmp_surv(2)];
       surv(3,2*i-1)=1; surv(3,2*i)=2;
  elseif (minIndex(3) == 3) %22 branch is survivor
       surv(3) = [tmp_surv(3)];
       surv(3,2*i-1)=2; surv(3,2*i)=2;
  else %32 branch is survivor
       surv(4) = [tmp_surv(4)];
       surv(3,2*i-1)=3; surv(3,2*i)=2;
  end
  %update state history table for state 3
  stateHist(3,i) = minIndex(3);
  %% STATE 3 %%
  %Calculate branch metrics going into state 3
  for (state=1:numStates)
       brMet(state,4) = (abs(chanOut(i) - h(1)*in(state) - h(2)*in(4))).^2;
       %Calculate partial metrics going into state 3
       tmpPartMet(4,state) = partMet(state) + brMet(state,4);
  end
  %update survivors
  [minVal(4), minIndex(4)] = min([tmpPartMet(4,1) tmpPartMet(4,2)
tmpPartMet(4,3)
tmpPartMet(4,4)]);
  if (minIndex(4) == 1) %03 branch is survivor
       surv(4) = [tmp_surv(1)];
       surv(4,2*i-1)=0; surv(4,2*i)=3;
  elseif (minIndex(4) == 2) %13 branch is survivor
       surv(4) = [tmp_surv(2)];
       surv(4,2*i-1)=1; surv(4,2*i)=3;
  elseif (minIndex(4) == 3) %23 branch is survivor
       surv(4) = [tmp_surv(3)];
       surv(4,2*i-1)=2; surv(4,2*i)=3;
  else %33 branch is survivor
       surv(4) = [tmp_surv(4)];
       surv(4,2*i-1)=3; surv(4,2*i)=3;
  end
  %update state history table for state 3
  stateHist(4,i) = minIndex(4);
  for (state=1:numStates)
     %update the temporary survivors
     tmp_surv(state) = surv(state);
     %update the partial metrics
     partMet(state) = minVal(state);
  end
end %end for
% Starting from the end of the trellis, work backwards to determine the state
transition
% sequence
for (i=size(msg,1):-1:2)
   stateSeq(i-1) = stateHist(stateSeq(i),i-1);
end
% States are from 0 to 3, not 1 to 4.
stateSeq = stateSeq-1;
% Traceback decoding. For each state, determine the input that led to that state
based
% on the current state and the previous state.
for (i=1:frameLength)
   switch (stateSeq(i))
   case 0
    switch (stateSeq(i+1))
    case 0
      decoded(i)=0;
    case 1
```

```
      decoded(i)=1;
    case 2
      decoded(i)=2;
    otherwise
      decoded(i)=3;

   end
    case 1
       switch (stateSeq(i+1))
       case 0
          decoded(i)=0;
       case 1
          decoded(i)=1;
    case 2
          decoded(i)=2;
    otherwise
          decoded(i)=3;
    end
       case 2
        switch (stateSeq(i+1))
        case 0
          decoded(i)=0;
      case 1
          decoded(i)=1;
      case 2
          decoded(i)=2;
      otherwise
          decoded(i)=3;
      end
      otherwise
      switch (stateSeq(i+1))
      case 0
          decoded(i)=0;
      case 1
          decoded(i)=1;
      case 2
          decoded(i)=2;
      otherwise
          decoded(i)=3;
       end
     end
   end
end %end if(0/1)

.
.
.
```